cmgh
CELLULAR AND MOLECULAR GASTROENTEROLOGY AND HEPATOLOGY

ORIGINAL RESEARCH

Oral Glucose Mobilizes Triglyceride Stores From the Human Intestine

Changting Xiao,[1] Priska Stahel,[1] Alicia L. Carreiro,[2] Yu-Han Hung,[2] Satya Dash,[1] Ian Bookman,[3] Kimberly K. Buhman,[2] and Gary F. Lewis[1]

[1]Division of Endocrinology and Metabolism, Departments of Medicine and Physiology, Banting and Best Diabetes Centre, University of Toronto, Toronto, Ontario, Canada; [2]Department of Nutrition Science, Purdue University, West Lafayette, Indiana; and [3]Kensington Screening Clinic, Toronto, Ontario, Canada

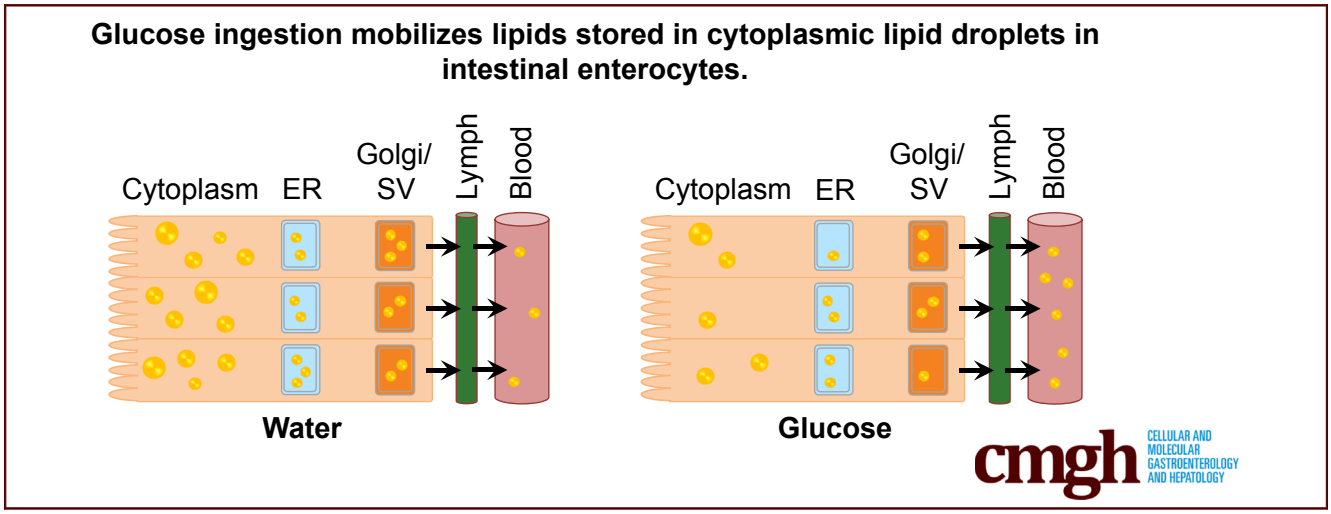

SUMMARY

Triglycerides are retained in the human gut long after ingestion of dietary fat. Oral glucose subsequently mobilizes triglyceride stores from the gut by recruiting cytoplasmic lipid droplets for chylomicron synthesis and secretion.

BACKGROUND & AIMS: The small intestine regulates plasma triglyceride (TG) concentration. Within enterocytes, dietary TGs are packaged into chylomicrons (CMs) for secretion or stored temporarily in cytoplasmic lipid droplets (CLDs) until further mobilization. We and others have shown that oral and intravenous glucose enhances CM particle secretion in human beings, however, the mechanisms through which this occurs are incompletely understood.

METHODS: Two separate cohorts of participants ingested a high-fat liquid meal and, 5 hours later, were assigned randomly to ingest either a glucose solution or an equivalent volume of water. In 1 group (N = 6), plasma and lipoprotein TG responses were assessed in a randomized cross-over study. In a separate group (N = 24), duodenal biopsy specimens were obtained 1 hour after ingestion of glucose or water. Ultrastructural and proteomic analyses were performed on duodenal biopsy specimens.

RESULTS: Compared with water, glucose ingestion increased circulating TGs within 30 minutes, mainly in the CM fraction. It decreased the total number of CLDs and the proportion of large-sized CLDs within enterocytes. We identified 2919 proteins in human duodenal tissue, 270 of which are related to lipid metabolism and 134 of which were differentially present in response to glucose compared with water ingestion.

CONCLUSIONS: Oral glucose mobilizes TGs stored within enterocyte CLDs to provide substrate for CM synthesis and secretion. Future studies elucidating the underlying signaling pathways may provide mechanistic insights that lead to the development of novel therapeutics for the treatment of hypertriglyceridemia. *(Cell Mol Gastroenterol Hepatol 2019;7:313–337; https://doi.org/10.1016/j.jcmgh.2018.10.002)*

Keywords: Intestine; Glucose; Triglycerides; Cytoplasmic Lipid Droplets.

Abbreviations used in this paper: **CLD, cytoplasmic lipid droplet; CM, chylomicron; ER, endoplasmic reticulum; FA, fatty acid; GLP-2, glucagon-like peptide-2; GO, Gene Ontology; SNARE, soluble *N*-ethylmaleimide-sensitive factor attachment protein receptor; TG, triglyceride; TRL, triglyceride-rich lipoprotein; VLDL, very-low-density lipoprotein.**

Most current article

2352-345X
https://doi.org/10.1016/j.jcmgh.2018.10.002

See editorial on page 291.

Hypertriglyceridemia, resulting from accumulation of circulating triglyceride (TG)-rich lipoprotein (TRL) particles in both fasting and postprandial states, is a highly prevalent condition and a significant risk factor for cardiovascular disease.[1] TGs, the main form of dietary fat, are hydrolyzed into fatty acids (FAs), glycerol, and monoglycerides by digestive enzymes in the intestinal lumen. These digestive products of dietary TGs are taken up by absorptive cells of the small intestine (enterocytes), where the majority of re-esterified TG is packaged into chylomicrons (CMs) and secreted into the circulation via the lymphatic system.[2] There is increasing evidence that, beyond the dominant regulation by lipid substrate availability, the intestine actively participates in the regulation of whole-body lipid metabolism via nutrient, hormonal, metabolic, and neural regulatory pathways.[3]

Aside from rapid TG incorporation into CMs, the intestine can store a considerable quantity of fat for several hours after the absorptive phase.[4] Studies in human beings suggest that dietary lipids originating from an earlier high-fat meal may contribute to CM TG after prolonged storage in the gut.[5–8] In addition, abundant lipid droplets are detected in human enterocytes 6 hours after ingestion of a high-fat liquid meal,[9] and in mice up to 12 hours after an oral fat gavage.[10] The exact site(s) of retained intestinal lipid stores and the quantity stored in each location have not been well characterized. Lipid droplets have been visualized in the cytoplasm of jejunal enterocytes in human beings[9] and mice,[10] and CMs have been observed in intracellular secretory pathways, in the lamina propria, and lacteals of the mesenteric lymphatics in human beings[9] and rodents.[10–12] Cytoplasmic lipid droplets (CLDs) are the best studied of these various lipid pools with respect to lipid storage and mobilization. CLDs consist of a neutral lipid core surrounded by a phospholipid monolayer. Numerous CLD-associated proteins have been identified and several have been shown to regulate CLD storage and metabolism.[13,14] The exact role of CLDs in the process of dietary fat absorption and their contribution to CM assembly and secretion is unknown, but studies in mice have indicated that CLD stores undergo dynamic changes in response to a dietary fat challenge.[15] Therefore, it is thought that CLDs may function as a temporary storage pool of neutral lipids for incorporation in CMs at later time points.[16,17]

Various dietary and hormonal factors play a role in mobilizing TGs stored within enterocytes from a previous meal. Several stimuli, including mixed meals,[18] glucose ingestion,[9] the gut hormone glucagon-like peptide-2 (GLP-2),[19] and sham fat feeding,[8] may trigger the mobilization of intestinal lipid stores. Ingestion of a mixed meal after a previous high-fat meal has been shown to elicit a peak in plasma TGs before the absorption of lipid from the current meal.[20] Glucose ingestion 5 hours after a high-fat meal decreases lipid stores in human enterocytes.[9] In healthy men, under the conditions of constant intraduodenal feeding and a pancreatic clamp, subcutaneous injection of GLP-2 caused a rapid and transient increase in plasma TGs and TRL particles.[19] In the latter study we showed that GLP-2 mobilized lipid that was ingested 7 hours earlier, which likely was retained in 1 or more of the earlier-mentioned intestinal lipid pools.[19] Furthermore, sham fat feeding was shown to stimulate CM secretion, suggesting the involvement of a neural regulatory pathway in intestinal lipid mobilization.[8] Collectively, mounting evidence supports the existence of TG stores in the human intestine that are subject to release in response to certain stimuli. However, the specific mechanism(s) by which mobilization of intestinal TG stores occurs remain unclear.

The goal of this study was to investigate the mechanism by which oral glucose mobilizes TGs stored within enterocytes in human beings and to identify the specific lipid pools that are mobilized. In each experiment, participants ingested a high-fat liquid meal and, 5 hours later, ingested glucose or water. In aim 1, in vivo circulating lipid responses to oral glucose were examined. In aim 2, duodenal biopsy specimens were obtained and ultrastructural and molecular responses were characterized.

Results

Oral Glucose Ingested 5 Hours After a High-Fat Liquid Meal Acutely Increases Plasma TG Concentration

Lipid responses to oral glucose and water were measured in 6 healthy participants (Table 1) in a study design illustrated in Figure 1*A*. As anticipated in aim 1, plasma glucose levels increased in response to the ingestion of glucose, but not water (Figure 1*B*). After glucose ingestion, plasma insulin levels also increased from a basal level of approximately 30 pmol/L to peak at approximately 150 pmol/L at 30 minutes, followed by a gradual decline to basal level 2 hours later (Figure 1*C*). In both groups plasma TGs increased to a postprandial peak at approximately 3 hours after fat ingestion before decreasing toward baseline (Figure 1*D*). With water ingestion, the decrease in plasma TGs continued unabated and approached basal levels at approximately 7 hours. However, after glucose ingestion, plasma TGs plateaued during the following 2 hours ($P = .024$ glucose vs water).

Oral Glucose Ingested 5 Hours After a High-Fat Liquid Meal Increased TGs in Total and CM-Sized, but Not in Smaller Very-Low-Density Lipoprotein–Sized, TRL Particles in the Circulation

Circulating total TRL TG tended to be higher after glucose vs water ingestion ($P = .091$) (Figure 1*E*). To identify whether large or small TRLs were most responsible for the increase in plasma and TRL TGs after glucose ingestion, TRLs were separated further by ultracentrifugation into larger CM-sized particles (Svedberg flotation > 400, predominantly comprising CMs) and smaller very-low-density lipoprotein (VLDL)-sized particles (Svedberg flotation 20–400, likely comprising both hepatically derived VLDL particles and smaller, intestinally derived CMs). An increase in TGs in the larger CM-sized TRL particles was observed with glucose ingestion ($P = .049$, analysis of variance) (Figure 1*F*). Despite interindividual variations, as is the usual

Table 1. Demographics and Biochemical Characteristics of Aim 1 Participants

Subject	Age, *y*	Weight, *kg*	Height, *cm*	BMI, *kg/m²*	Waist, *cm*	Fasting glucose level, *mmol/L*	Fasting TG level, *mmol/L*	Fasting insulin level, *pmol/L*
1	58	72	178	23	95.5	5.6	0.76	35
2	46	77	166	27	101	4.9	0.73	48
3	46	87	182	26	100	4.5	0.97	37
4	53	76	172	25.7	87	4.9	1.99	94
5	29	87	182	26.4	94	4.4	0.68	36.5
6	57	84	179	26	88	4.5	0.59	29
Means	48.2	80.5	176.5	25.7	94.3	4.8	1.0	46.6
SE	4.4	2.6	2.6	0.6	2.4	0.2	0.2	9.8

BMI, body mass index.

case for most human mechanistic studies, the response was statistically significant because each subject showed a response to glucose, either a reversal of the decrease or an attenuated decrease. Changes in the smaller VLDL-sized TRL particles were similar with both glucose and water ingestion ($P = .340$) (Figure 1*G*). These results suggest that the increase in plasma TGs in response to glucose ingestion was owing exclusively to an increase in CM-sized TRL particles.

Presence of Lipid Pools Within the Intestinal Mucosa

Duodenal biopsy specimens were obtained 1 hour after glucose or water ingestion from 24 participants (Table 2). Enterocytes within biopsy specimens were subjected to ultrastructural analysis using transmission electron microscopy. Consistent with previous observations, the duodenal samples obtained 6 hours after fat ingestion contained considerable quantities of lipids both intracellularly and extracellularly (Figure 2*A*). Within enterocytes, lipids were observed in large CLDs (Figure 2*B*), in smaller lipid droplets within the endoplasmic reticulum (ER) (Figure 2*C*), and within the Golgi (Figure 2*D*). In addition, secreted CMs were present in the intercellular spaces between enterocytes. Overall, the enterocyte ultrastructure and lipid pools observed in human duodenal enterocytes appeared similar to what has been observed previously in mice.[12]

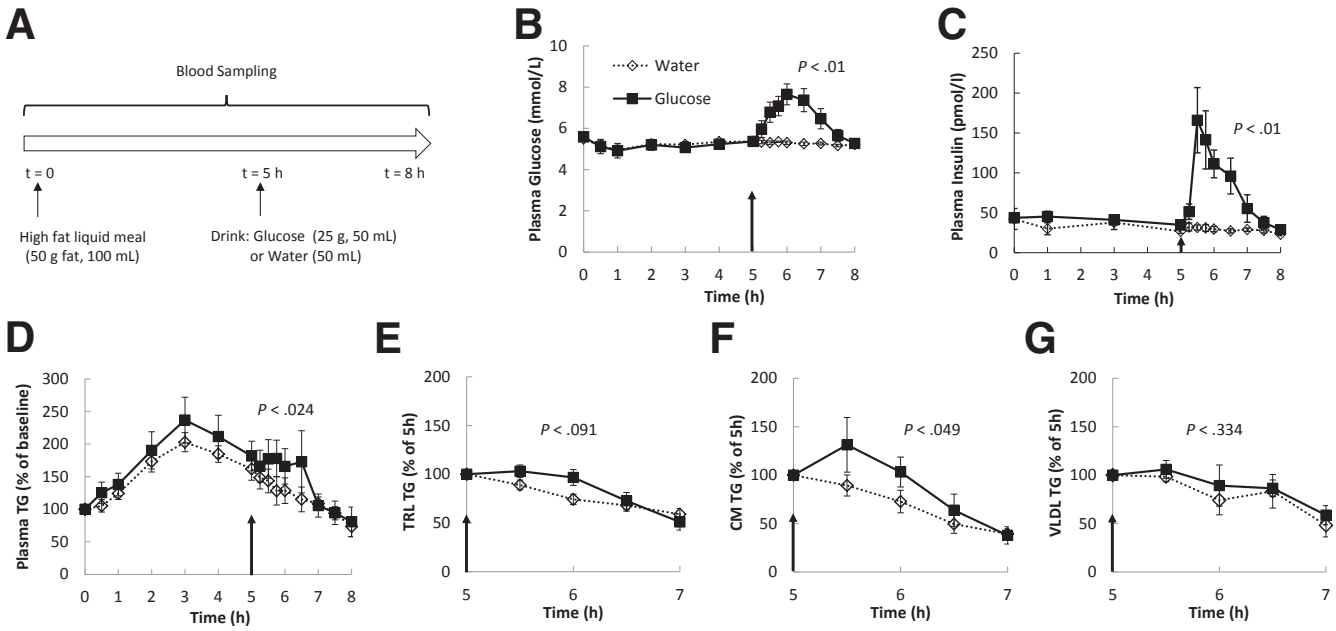

Figure 1. Lipid responses to oral glucose ingestion. (*A*) Study design. After an overnight fast, subjects ingested a high-fat liquid meal and 5 hours later ingested a glucose solution or equivalent volume of water in 2 randomized visits. (*B*) Blood glucose and (*C*) insulin concentrations during the study period. (*D*) TG concentrations in plasma during the study period, expressed as a percentage of baseline. (*E–G*) TG concentrations in total TRL, CM-sized TRL, and VLDL-sized TRL 2 hours after glucose or water ingestion, expressed as the percentage of levels at t = 5 hours. *Arrows* indicate time of glucose or water ingestion. All *P* values were with repeated-measures analysis of variance between 5 and 7 hours.

Table 2. Demographics of Aim 2 Participants

	Glucose	Placebo
N	12	12
BMI, kg/m^2	25.3 ± 0.9	25.5 ± 1.5
Age, *y*	34.6 ± 2.9	34.7 ± 3.1
Sex	4 M/8 F	2 M/10 F

NOTE. Data are means ± SE for BMI and age.
BMI, body mass index; F, female; M, male.

Oral Glucose Mobilizes Enterocyte CLD Stores

We performed quantitative analyses of enterocyte CLDs in duodenal biopsy specimens obtained in a design similar to that of aim 1 (Figure 3*A*). After glucose and water ingestion, 34% and 44% of enterocytes per biopsy sample contained CLDs, respectively (Figure 3*B*) ($P = .14$). In the samples containing CLDs, there were fewer CLDs per cell in response to glucose compared with water (Figure 3*C*) ($P = .02$). Although the average diameters ($P = .18$) and areas ($P = .17$) of individual CLDs were not significantly different between treatments (data not shown), there were differences in the CLD diameter distributions, with more CLDs falling into the smaller size ranges and fewer into larger size ranges after glucose compared with water ingestion (Figure 3*D*) ($P = .03$). However, the difference between treatments in total CLD area per enterocyte did not reach statistical significance (Figure 3*E*) ($P = .11$). We also assessed the amount of lipids within the secretory pathway in enterocytes, which included lipids in the ER, Golgi, and Golgi-derived secretory vesicles. There were no significant differences in the proportion of biopsy specimens containing low, moderate, and high amounts of secretory lipids in response to glucose compared with water ingestion (Figure 3*F*) ($P = .29$, Fisher exact test). Taken together, glucose ingestion resulted in fewer CLDs in enterocytes and a shift toward smaller-sized CLDs.

Oral Glucose Does Not Mobilize Lipids Within Enterocytes After Delayed Fasting

To investigate whether glucose mobilization of intestinal lipid stores persists after more prolonged fasting, a separate group of subjects (Table 3) ingested glucose or water 9 hours after the high-fat liquid meal. Duodenal biopsy specimens were collected 1 hour later (10 hours after ingesting the high-fat liquid meal). Under these conditions, no stimulatory effect of glucose on lipid mobilization was observed. There were no significant differences in the percentage of cells with CLDs, CLD number or size, or in the amount of lipids within the secretory pathway in enterocytes in

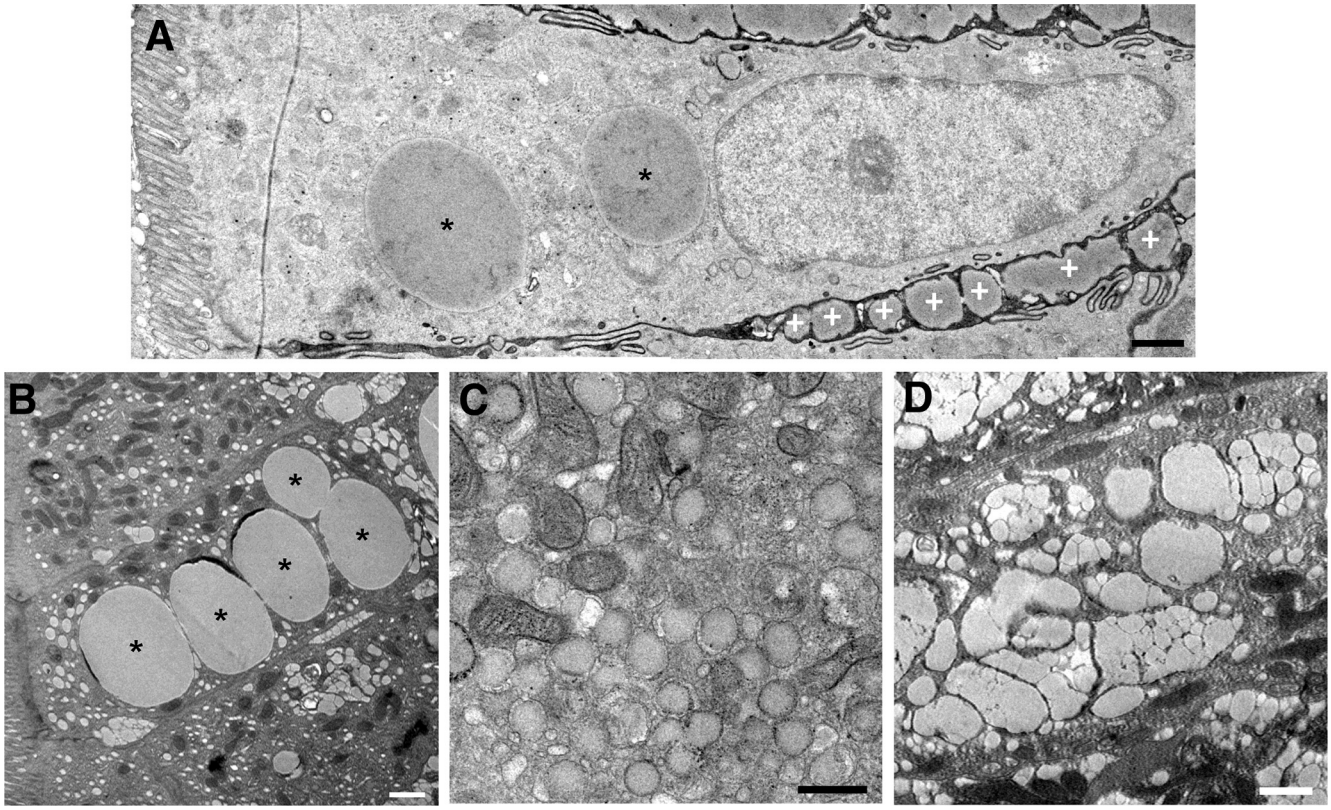

Figure 2. Lipid pools within the intestinal mucosa. (*A*) A transmission electron microscopy image of an enterocyte from a duodenal biopsy specimen obtained 6 hours after a high-fat liquid meal and 1 hour after glucose ingestion. Lipid present within CLDs is shown (*asterisk*), as well as in secreted CMs in the intercellular space (*white plus symbol*). (*B*) An enterocyte containing lipid within several large CLDs (*asterisk*). (*C*) An enterocyte containing lipid within smaller lipid droplets in the ER, which are surrounded by a bilayer membrane and usually are observed at the apical side of the cell. (*D*) Lipid present within the Golgi of an enterocyte, which normally was observed above the nucleus. *Scale bars*: 1 μm (*A*, *B*, and *D*), and 0.5 μm (*C*).

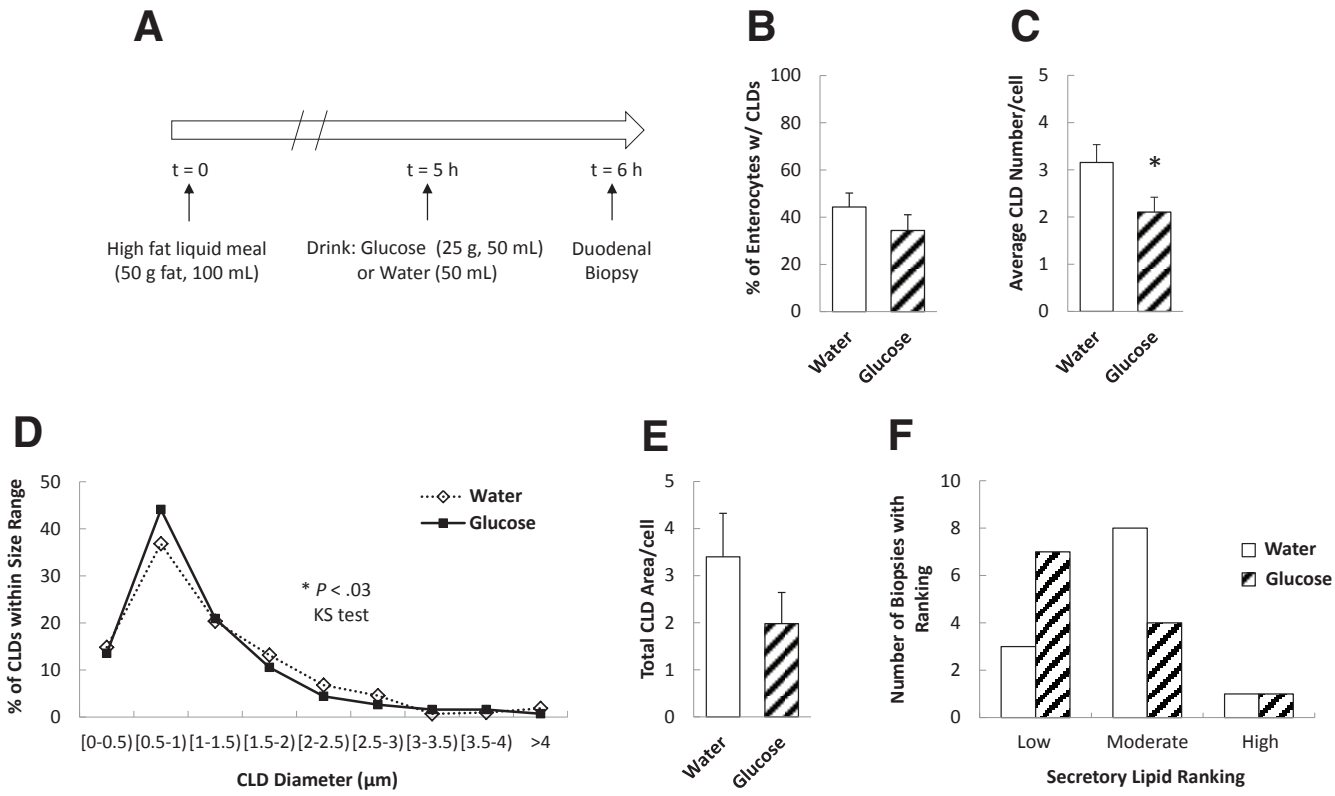

Figure 3. Oral glucose mobilizes enterocyte CLD stores. (*A*) Study design. Enterocyte CLD and secretory lipid stores were analyzed 6 hours after a high-fat liquid meal and 1 hour after glucose or water ingestion (N = 12 patients per group). (*B*) Percentage of enterocytes containing CLDs ($P = .14$, *t* test). (*C*) Average CLD number per cell ($P = .022$, *t* test). (*D*) CLD diameter distribution ($P = .03$, Kolmogorov–Smirnov test) and (*E*) average total CLD area per cell ($P = .11$, *t* test). (*F*) Amount of lipid within the secretory pathway (includes lipid in ER, Golgi, and secretory vesicles) ($P = .29$ Fisher exact test).

response to glucose compared with water ingestion (Figure 4). This likely was owing to a lower proportion of enterocytes containing CLDs after prolonged fasting compared with the 6-hour fast (Figure 5). Thus, mobilization of enterocyte CLDs by oral glucose appears to depend on the presence of a sufficient pool of intestinal lipid stores retained in the enterocyte after fat ingestion.

Differential Expression of Proteins in Duodenal Biopsy Specimens From Subjects Administered Glucose or Water After a High-Fat Liquid Meal

Untargeted proteomic analysis of duodenal biopsy specimens identified 2919 proteins, with 2900 present in both water and glucose ingestion conditions, only 9 were identified in response to glucose and only 10 were identified in response to water ingestion (Figure 6*A*). A total of 48 of these proteins were present at relatively lower levels and 86 were present at relatively higher levels in response to glucose compared with water (Table 4). After correction for multiple statistical tests, the relative levels of 7 proteins remained significantly different between treatments.

The differentially expressed proteins (defined as $P < .05$ between treatment groups) were classified into broad groups based on gene ontology (GO) terms for biological processes and molecular functions (Table 5, Figure 6*B*). Among the 48 proteins present at relatively lower levels in response to glucose, protein folding/transport (19%), immune response (15%), and transcription/RNA processing/translation (15%) were the most abundant functions. Of the 86 proteins present at relatively higher levels in response to glucose, those involved in protein metabolism (21%), mitochondria/redox (16%), and transcription/RNA processing/translation (15%) were the most abundant. Interestingly, in response to glucose compared with water ingestion, histone proteins were present at relatively lower levels, while those involved in carbohydrate metabolism, ion transport, and lipid metabolism all were present at relatively higher levels.

Table 3. Demographics of Additional Participants Participating in Aim 2 With Delayed Fasting

	Glucose	Placebo
N	5	5
BMI, kg/m^2	23.8 ± 1.2	22.2 ± 1.4
Age, *y*	33.0 ± 3.8	33.6 ± 3.2
Sex	1 M/4 F	1 M/4 F

NOTE. Data are means ± SE for BMI and age.
BMI, body mass index; F, female; M, male.

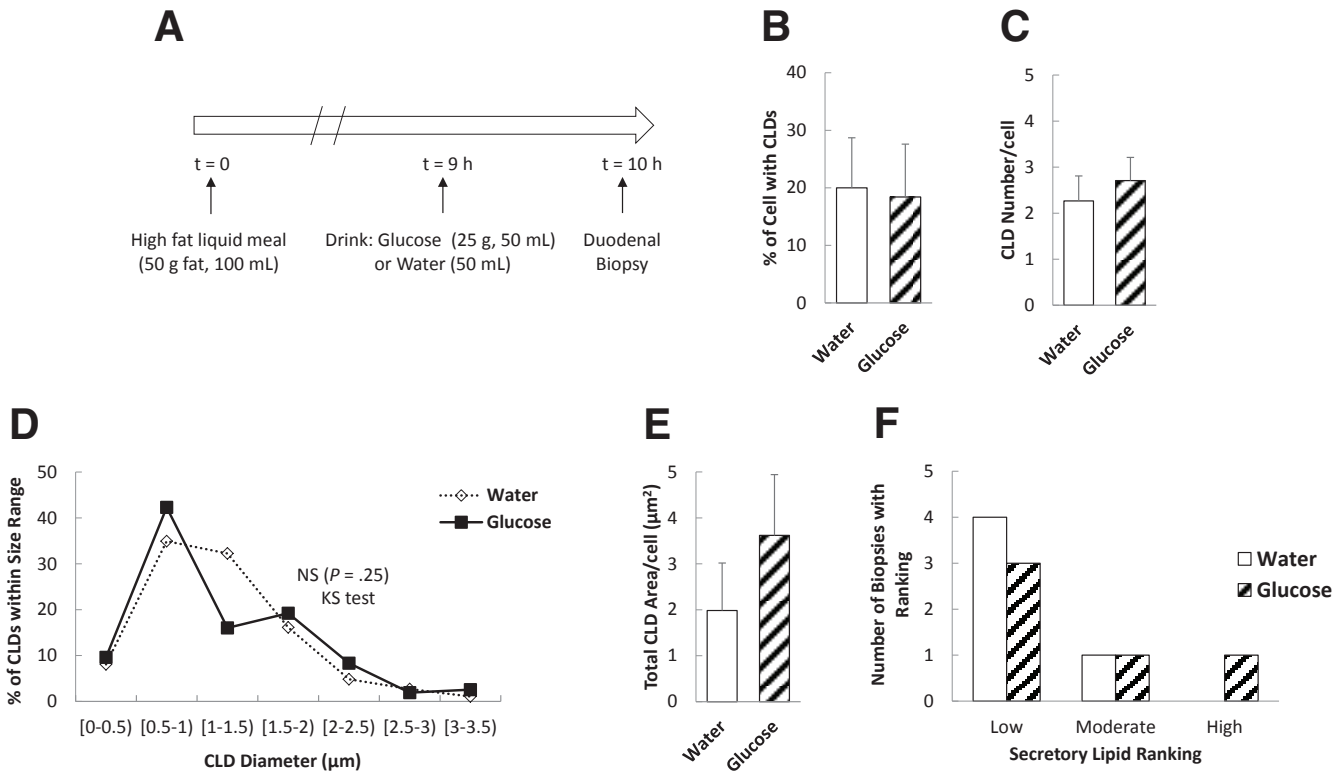

Figure 4. Analysis of enterocyte lipid stores in response to glucose or water ingestion after a delayed fast. (*A*) Study design. Duodenal biopsy specimens were obtained 10 hours after ingestion of a high-fat liquid meal and 1 hour after ingestion of glucose or water. (*B*) Percentage of enterocytes containing CLDs ($P = .45$). (*C*) Average CLD number per cell ($P = .28$). (*D*) CLD diameter distribution and (*E*) average total CLD area per cell ($P = .18$). (*F*) Amount of lipid within the secretory pathway (includes lipid in ER, Golgi, and secretory vesicles) ($P = 1$, Fisher exact test). Average CLD number and total CLD area per cell were compared with a *t* test.

Because our goal was to identify mechanisms by which intestinal lipid stores are mobilized in response to glucose ingestion, we then specifically examined lipid metabolism-related proteins. Of the 2919 proteins identified, 270 (9%) are known to be involved in lipid/lipoprotein metabolism and transport. The majority of these proteins are involved in FA modification, metabolism, and transport (32%, cluster 4) and lipoprotein metabolism (23%, cluster 2); however, proteins involved in cholesterol/steroid metabolism (cluster 3), TG/phospholipid metabolism (cluster 1), lipid binding,

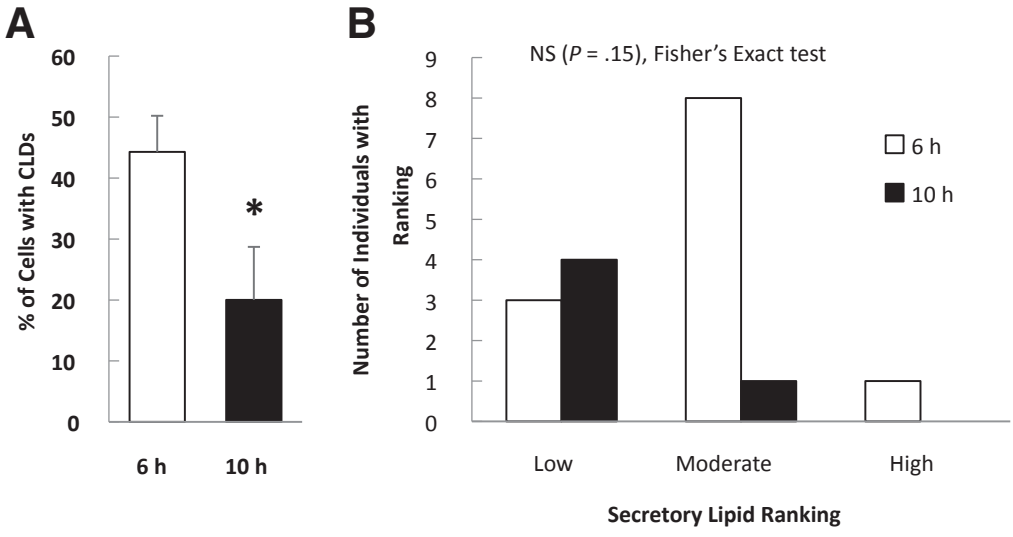

Figure 5. Comparison of enterocyte lipid stores after different fasting times. (*A*) Percentage of cells containing CLDs ($P = .025$) and (*B*) amount of lipid within the secretory pathway ($P = .15$, Fisher exact test) in individuals at 6 hours compared with 10 hours after the high-fat liquid meal (and 1 h after water consumption). *$P < .05$, *t* test.

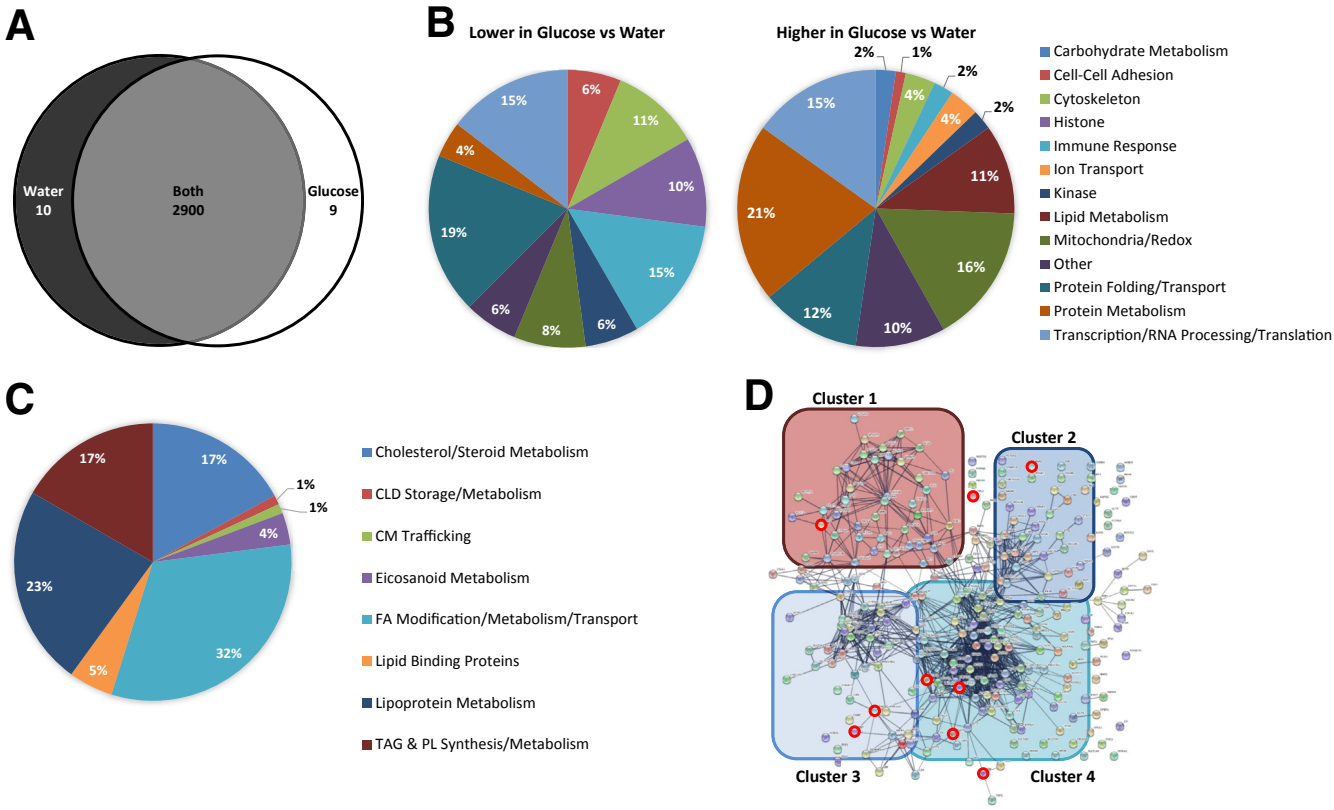

Figure 6. Proteins present in duodenal biopsy specimens from subjects administered glucose or water after a high-fat liquid meal. Duodenal biopsy specimens were collected 6 hours after lipid and 1 hour after glucose or water ingestion from patients undergoing a diagnostic endoscopy (N = 12 patients per group). (*A*) Venn diagram of proteins identified in response to glucose or water ingestion. Proteins present in at least 3 samples in 1 group and 0 samples in the other group were considered present in only 1 group. Proteins identified in at least 3 samples in 1 group and at least 1 sample in the other group were considered present in both groups. (*B*) Percentage of proteins within broad functional groups that were present at either relatively lower (48 total proteins) or relatively higher (86 total proteins) levels in response to glucose compared with water ingestion, as classified based on their biological/molecular functions. Only proteins that were identified in at least 3 samples in both groups and present at relatively different levels ($P < .05$, *t* test), or at least 3 samples in 1 group and 0 samples in the other group, were included in this classification. A Database for Annotation, Visualization, and Integrated Discovery search of the 2919 identified proteins resulted in the identification of 270 proteins with GO terms related to lipid metabolism. (*C*) Percentage of the 270 lipid metabolism-related proteins involved in more specific lipid-related functions. (*D*) String analysis of the 270 lipid metabolism-related proteins. The thickness of the *line* represents the strength of evidence of a structural/functional relationship between 2 proteins. Cluster 1 is enriched in proteins involved in TG and phospholipid (PL) synthesis and metabolism, cluster 2 is enriched in proteins involved in lipoprotein metabolism, cluster 3 is enriched in proteins involved in cholesterol/steroid metabolism, and cluster 4 is enriched in proteins involved in FA modification/metabolism/transport. Proteins that were present at relatively different levels in response to glucose compared with water consumption ($P < .05$, *t* test) are *circled in red*. TAG, triacylglycerol.

eicosanoid metabolism, CLD storage/metabolism, and CM trafficking also were identified (Figure 6*C* and *D*). In response to glucose compared with water ingestion, 9 of these lipid-related proteins were present at relatively higher levels ($P < .05$) (Table 6). Of note, ethanolaminephosphotransferase 1 was identified only in response to glucose ingestion.

A similar comparative proteomic analysis was performed in response to glucose or water ingestion after a longer, overnight fast after the ingestion of a high-fat meal (samples collected 10 hours after a high-fat meal and 1 hour after glucose/water ingestion), in which there were no observed differences in enterocyte CLD stores. This analysis identified 1683 proteins, with 1673 common to both groups, 9 identified only in response to water, and 1 identified only in response to glucose ingestion (Figure 7*A*). The 96 proteins that were differentially present in this analysis are involved in a variety of cellular processes, with a greater proportion of proteins associated with transcription and translation (GO terms) compared with the initial study (Tables 7 and 8, Figure 7*B*). The 186 lipid metabolism-related proteins identified in this analysis are involved in similar processes as the initial study (Figure 7*C* and *D*); however, none of the 6 lipid metabolism proteins that were differentially present in response to glucose compared with water ingestion were the same as those identified at 6 hours after ingesting a high-fat meal (Table 9).

Table 4. Proteins Present at Relatively Different Levels in Duodenal Biopsy Specimens From Subjects Administered Glucose or Water After a High-Fat Liquid Meal

Uniprot accession	Protein name	Gene name	Fold change	*t* test *P* value	Function
P05997	Collagen α-2(V) chain[a]	COL5A2	-7.4957	.0030	Other (extracellular matrix protein)
Q5T5C0	Syntaxin-binding protein 5[a]	STXBP5	-6.8628	4.72E-22	Protein folding/transport
Q8N2S1	Latent-transforming growth factor β-binding protein 4[a]	LTBP4	-6.7854	.0002	Protein folding/transport
O14672	Disintegrin and metalloproteinase domain-containing protein 10[a]	ADAM10	-6.7264	.0010	Protein metabolism
P17480	Nucleolar transcription factor 1[a]	UBTF	-6.2100	.0063	Transcription/RNA processing/translation
Q8N8S7	Protein enabled homolog[a]	ENAH	-5.7620	.0007	Cytoskeleton
Q7Z6K5	Arpin[a]	ARPIN	-5.7573	2.02E-19	Cytoskeleton
Q9UQ35	Serine/arginine repetitive matrix protein 2[a]	SRRM2	-5.5687	.0002	Transcription/RNA processing/translation
P49790	Nuclear pore complex protein Nup153[a]	NUP153	-5.1794	.0079	Transcription/RNA processing/translation
Q9NRG7	Epimerase family protein SDR39U1[a]	SDR39U1	-4.1142	3.26E-28	Mitochondria/redox
P16403	Histone H1.2	HIST1H1C	-1.0513	.0213	Histone
P01860	Immunoglobulin heavy constant γ 3	IGHG3	-1.0063	.0007	Immune response
P13284	γ-interferon–inducible lysosomal thiol reductase	IFI30	-1.0048	.0116	Mitochondria/redox
P35580	Myosin-10	MYH10	-0.9176	.0449	Cytoskeleton
P08590	Myosin light chain 3	MYL3	-0.8947	.0464	Other (regulation of muscle contraction)
Q71UI9	Histone H2A.V	H2AFV	-0.8933	.0072	Histone
Q71DI3	Histone H3.2		-0.8572	.0338	Histone
A0A0B4J1X5	Immunoglobulin heavy variable 3–74	IGHV3-74	-0.8112	.0076	Immune response
Q99829	Copine-1	CPNE1	-0.7877	.0101	Transcription/RNA processing/translation
P01780	Immunoglobulin heavy variable 3–7	IGHV3-7	-0.7127	.0154	Immune response
P42167	Lamina-associated polypeptide 2; isoforms β/γ	TMPO	-0.6933	.0453	Cell–cell adhesion
P0CG06	Immunoglobulin λ constant 2	IGLC2	-0.6852	.0260	Immune response
Q96KA5	Cleft lip and palate transmembrane protein 1–like protein	CLPTM1L	-0.6539	.0031	Other (apoptosis)
P01859	Immunoglobulin heavy constant γ 2	IGHG2	-0.6532	.0234	Immune response
P84243	Histone H3.3	H3F3A	-0.6487	.0236	Histone
Q8IUX7	Adipocyte enhancer-binding protein 1	AEBP1	-0.637	.0226	Transcription/RNA processing/translation
Q09666	Neuroblast differentiation-associated protein AHNAK	AHNAK	-0.635	.0397	Cell–cell adhesion
Q9BY50	Signal peptidase complex catalytic subunit SEC11C	SEC11C	-0.6182	.0288	Protein metabolism
P07305	Histone H1.0	H1F0	-0.5824	.0446	Histone
P01857	Immunoglobulin heavy constant γ 1	IGHG1	-0.5542	.0206	Immune response
Q9UEW8	STE20/SPS1-related proline-alanine–rich protein kinase	STK39 SPAK	-0.5436	.0033	Kinase
P30405	Peptidyl-prolyl cis-trans isomerase F; mitochondrial	PPIF	-0.5252	.0168	Protein folding/transport
P56378	6.8-kilodalton mitochondrial proteolipid	MP68	-0.4738	.0418	Mitochondria/redox
P61758	Prefoldin subunit 3	VBP1	-0.4401	.0427	Protein folding/transport
Q96L92	Sorting nexin-27	SNX27	-0.427	.0158	Protein folding/transport
O75323	Protein NipSnap homolog 2	GBAS	-0.4059	.0315	Mitochondria/redox

Table 4. Continued

Uniprot accession	Protein name	Gene name	Fold change	*t* test *P* value	Function
O75190	DnaJ homolog subfamily B member 6	DNAJB6	-0.3578	.0384	Protein folding/transport
Q86UP2	Kinectin	KTN1	-0.3174	.0401	Cell–cell adhesion
Q15629	Translocating chain-associated membrane protein 1	TRAM1	-0.3048	.0452	Protein folding/transport
Q9BWS9	Chitinase domain-containing protein 1	CHID1	-0.2768	.0223	Immune response
O00186	Syntaxin-binding protein 3	STXBP3	-0.2611	.0332	Protein folding/transport
Q02543	60S ribosomal protein L18a	RPL18A	-0.2238	.0089	Transcription/RNA processing/translation
P13861	cAMP-dependent protein kinase type II-α regulatory subunit	PRKAR2A	-0.217	.0098	Kinase
P84085	ADP-ribosylation factor 5	ARF5	-0.1788	.0354	Protein folding/transport
P28482	Mitogen-activated protein kinase 1	MAPK1	-0.1528	.0078	Kinase
P59998	Actin-related protein 2/3 complex subunit 4	ARPC4	-0.1477	.0141	Cytoskeleton
O15145	Actin-related protein 2/3 complex subunit 3	ARPC3	-0.145	.0464	Cytoskeleton
Q5VTE0	Putative elongation factor 1-α–like 3	EEF1A1P5	-0.134	.0151	Transcription/RNA processing/translation
Q8IZ83	Aldehyde dehydrogenase family 16 member A1	ALDH16A1	0.1539	.0433	Mitochondria/redox
Q96A33	Coiled-coil domain-containing protein 47	CCDC47	0.1676	.0403	Other (calcium ion homeostasis, ERAD)
Q9NPA0	ER membrane protein complex subunit 7	EMC7	0.1744	.0474	Other (carbohydrate binding)
Q15417	Calponin-3	CNN3	0.1993	.0488	Cytoskeleton
P21281	V-type proton ATPase subunit B; brain isoform	ATP6V1B2	0.2023	.0460	Ion transport
P48556	26S proteasome non-ATPase regulatory subunit 8	PSMD8	0.209	.0347	Protein metabolism
O14734	Acyl-coenzyme A thioesterase 8	ACOT8	0.2101	.0177	Lipid metabolism
Q9NS69	Mitochondrial import receptor subunit TOM22 homolog	TOMM22	0.2105	.0281	Mitochondria/redox
P11940	Polyadenylate-binding protein 1	PABPC1	0.2111	.0441	Transcription/RNA processing/translation
P78344	Eukaryotic translation initiation factor 4 γ 2	EIF4G2	0.2114	.0490	Transcription/RNA processing/translation
Q14974	Importin subunit β-1	KPNB1	0.2177	.0417	Protein folding/transport
Q13200	26S proteasome non-ATPase regulatory subunit 2	PSMD2	0.2182	.0108	Protein metabolism
O95782	AP-2 complex subunit α-1	AP2A1	0.219	.0059	Protein folding/transport
Q93034	Cullin-5	CUL5	0.2198	.0058	Protein metabolism
Q9UNZ2	NSFL1 cofactor p47	NSFL1C	0.2214	.0150	Protein metabolism
Q9BTM9	Ubiquitin-related modifier 1	URM1	0.2221	.0047	Transcription/RNA processing/translation
O75436	Vacuolar protein sorting-associated protein 26A	VPS26A	0.2305	.0230	Protein folding/transport
P25788	Proteasome subunit α type-3	PSMA3	0.2323	.0358	Protein metabolism
Q9Y2Z0	Protein SGT1 homolog	SUGT1	0.2356	.0128	Protein metabolism
Q9P2J5	Leucine-tRNA ligase; cytoplasmic	LARS	0.2405	.0207	Transcription/RNA processing/translation
P38606	V-type proton ATPase catalytic subunit A	ATP6V1A	0.2418	.0123	Ion transport
Q93008	Probable ubiquitin carboxyl-terminal hydrolase FAF-X	USP9X	0.2423	.0467	Protein metabolism

Table 4. Continued

Uniprot accession	Protein name	Gene name	Fold change	*t* test *P* value	Function
P11142	Heat shock cognate 71-kilodalton protein	HSPA8	0.253	.0051	Protein folding/transport
P55060	Exportin-2	CSE1L	0.2541	.0385	Protein folding/transport
O75146	Huntingtin-interacting protein 1–related protein	HIP1R	0.259	.0285	Cytoskeleton
O96008	Mitochondrial import receptor subunit TOM40 homolog	TOMM40	0.2593	.0076	Mitochondria/redox
P15531	Nucleoside diphosphate kinase A	NME1	0.271	.0213	Kinase
P46734	Dual-specificity mitogen-activated protein kinase kinase 3	MAP2K3	0.2752	.0373	Kinase
P28070	Proteasome subunit β type-4	PSMB4	0.2764	.0158	Protein Metabolism
O75381	Peroxisomal membrane protein PEX14	PEX14	0.2803	.0238	Protein folding/transport
Q9NUQ8	ATP-binding cassette subfamily F member 3	ABCF3	0.2846	.0347	Cell–cell adhesion
Q9Y697	Cysteine desulfurase; mitochondrial	NFS1	0.2919	.0167	Protein metabolism
Q02790	Peptidyl-prolyl cis-trans isomerase FKBP4	FKBP4	0.2953	.0477	Protein folding/transport
Q15020	Squamous cell carcinoma antigen recognized by T cell 3	SART3	0.3007	.0457	Transcription/RNA processing/translation
Q01813	ATP-dependent 6-phosphofructokinase; platelet type	PFKP	0.3087	.0367	Carbohydrate metabolism
Q5H9R7	Serine/threonine-protein phosphatase 6 regulatory subunit 3	PPP6R3	0.3154	.0231	Protein metabolism
O95433	Activator of 90-kilodalton heat shock protein ATPase homolog 1	AHSA1	0.3177	.0091	Protein folding/transport
O00231	26S proteasome non-ATPase regulatory subunit 11	PSMD11	0.3221	.0158	Protein metabolism
P31689	DnaJ homolog subfamily A member 1	DNAJA1	0.3234	.0479	Protein folding/transport
O75915	PRA1 family protein 3	ARL6IP5	0.3236	.0439	Cytoskeleton
Q9ULA0	Aspartyl aminopeptidase	DNPEP	0.3283	.0271	Protein metabolism
Q99757	Thioredoxin; mitochondrial	TXN2	0.3371	.0343	Mitochondria/redox
Q9NTX5	Ethylmalonyl-CoA decarboxylase	ECHDC1	0.341	.0450	Lipid metabolism
Q96GK7	Fumarylacetoacetate hydrolase domain-containing protein 2A	FAHD2A	0.35	.0195	Other (potential hydrolase)
Q9Y3D9	28S ribosomal protein S23; mitochondrial	MRPS23	0.3593	.0114	Transcription/RNA processing/translation
P23526	Adenosylhomocysteinase	AHCY	0.3976	.0216	Other (regulation of methylation)
P18827	Syndecan-1	SDC1	0.4174	.0314	Other (cell migration)
P08621	U1 small nuclear ribonucleoprotein 70 kilodaltons	SNRNP70	0.4216	.0144	Transcription/RNA processing/translation
P28838	Cytosol aminopeptidase	LAP3	0.4431	.0436	Protein metabolism
Q9NR19	Acetyl-coenzyme A synthetase; cytoplasmic	ACSS2	0.4512	.0470	Lipid metabolism
Q8N5G0	Small integral membrane protein 20	SMIM20	0.4532	.0296	Mitochondria/redox
P49247	Ribose-5-phosphate isomerase	RPIA	0.4698	.0326	Carbohydrate metabolism
Q9Y333	U6 snRNA-associated Sm-like protein LSm2	LSM2	0.4741	.0355	Transcription/RNA processing/translation
Q9H490	Phosphatidylinositol glycan anchor biosynthesis class U protein	PIGU	0.4799	.0487	Lipid metabolism
O75382	Tripartite motif-containing protein 3	TRIM3	0.485	.0174	Immune response
Q15125	3-β-hydroxysteroid-Δ(8); Δ(7)-isomerase	EBP	0.4859	.0413	Lipid metabolism

Table 4. Continued

Uniprot accession	Protein name	Gene name	Fold change	*t* test *P* value	Function
Q16881	Thioredoxin reductase 1; cytoplasmic	TXNRD1	0.4905	.0148	Mitochondria/redox
P07108	Acyl-CoA binding protein	DBI	0.4917	.0382	Lipid metabolism
P48637	Glutathione synthetase	GSS	0.4944	.0440	Other (glutathione synthesis)
O76003	Glutaredoxin-3	GLRX3	0.4953	.0403	Mitochondria/redox
Q12882	Dihydropyrimidine dehydrogenase [NADP(+)]	DPYD	0.5076	.0165	Mitochondria/redox
Q9NWU5	39S ribosomal protein L22; mitochondrial	MRPL22	0.526	.0101	Transcription/RNA processing/translation
Q9NVS9	Pyridoxine-5'-phosphate oxidase	PNPO	0.5395	.0337	Mitochondria/redox
Q9UHY7	Enolase-phosphatase E1	ENOPH1	0.5544	.0307	Protein metabolism
P16930	Fumarylacetoacetase	FAH	0.5694	.0236	Protein metabolism
P48506	Glutamate-cysteine ligase catalytic subunit	GCLC	0.5745	.0241	Mitochondria/redox
Q8N983	39S ribosomal protein L43; mitochondrial	MRPL43	0.5932	.0266	Transcription/RNA processing/translation
Q9UBM7	7-dehydrocholesterol reductase	DHCR7	0.6045	.0283	Lipid metabolism
P48147	Prolyl endopeptidase	PREP	0.6099	.0244	Protein metabolism
P82673	28S ribosomal protein S35; mitochondrial	MRPS35	0.6118	.0363	Transcription/RNA processing/translation
Q8WVX9	Fatty acyl-CoA reductase 1	FAR1	0.6231	.0223	Lipid metabolism
Q9Y679	Ancient ubiquitous protein 1	AUP1	0.6292	.0093	Protein metabolism
P37840	α-synuclein	SNCA	0.6332	.0063	Mitochondria/redox
Q9BRF8	Serine/threonine-protein phosphatase CPPED1	CPPED1	0.6702	.0313	Protein metabolism
Q6UX53	Methyltransferase-like protein 7B	METTL7B	0.7067	.0210	Other (probable methyltransferase)
P02792	Ferritin light chain	FTL	0.8169	.0124	Ion transport
P02794	Ferritin heavy chain	FTH1	0.8959	.0144	Mitochondria/redox
Q9BVL4	Selenoprotein O[b]	SELENOO	5.0987	.0002	Mitochondria/redox
Q9HB07	UPF0160 protein MYG1; mitochondrial[b]	C12orf10	5.9843	5.8E-16	Mitochondria/redox
P22090	40S ribosomal protein S4[b]	RPS4Y1	6.7537	.0018	Transcription/RNA processing/translation
Q9P003	Protein cornichon homolog 4[b]	CNIH4	7.1618	1.74E-15	Protein folding/transport
O60938	Keratocan[b]	KERA	7.4582	.0050	Other (keratan sulfate metabolism/cornea development)
Q9C0D9	Ethanolaminephosphotransferase 1[b]	SELENOI	7.4638	.0005	Lipid metabolism
Q96HV5	Transmembrane protein 41A[b]	TMEM41A	7.5997	.0023	Other (transmembrane protein)
P62306	Small nuclear ribonucleoprotein F[b]	SNRPF	7.7847	3.21E-17	Transcription/RNA processing/translation
Q8NDA2	Hemicentin-2[b]	HMCN2	11.5204	3.81E-16	Immune response

NOTE. Proteins identified in at least 3 samples in both groups, or at least 3 samples in 1 group and 0 samples in the other group, were compared. Proteins present at significantly different levels within the 2 treatment groups ($P < .05$, *t* test) are shown. Average fold change of proteins in response to glucose relative to water consumption are presented. Numbers in the "Fold change" column represent how much higher (or lower if negative) the protein levels were in the glucose group compared with the water group. Proteins are listed in descending order according to relative fold change, with negative fold change values indicating relative down-regulation by glucose (listed at the top of the table) followed by those up-regulated by glucose indicated by a positive fold change (with greatest positive fold change listed at the bottom of table).
ADP, adenosine diphosphate; ATP, adenosine triphosphate; ATPase, adenosine triphosphatase; cAMP, cyclic adenosine monophosphate; ERAD, endoplasmic-reticulum-associated protein degradation; NADP, nicotinamide adenine dinucleotide phosphate; redox, reduction-oxidation; tRNA, transfer ribonucleic acid.
[a]Only identified in response to water.
[b]Only identified in response to glucose.

Table 5. GO Terms Associated With Lipid Metabolism-Related Proteins Present in Duodenal Biopsy Specimens 6 Hours After a High-Fat Liquid Meal

Cholesterol/steroid metabolism	
UP_KEYWORDS	Cholesterol biosynthesis
GOTERM_BP_DIRECT	Cholesterol biosynthetic process
UP_KEYWORDS	Cholesterol metabolism
UP_KEYWORDS	Steroid biosynthesis
KEGG_PATHWAY	Steroid hormone biosynthesis
UP_KEYWORDS	Steroid metabolism
UP_KEYWORDS	Sterol biosynthesis
GOTERM_MF_DIRECT	Sterol esterase activity
UP_KEYWORDS	Sterol metabolism
CLD storage/metabolism	
GOTERM_CC_DIRECT	Lipid droplet
GPTERM_BP_DIRECT	Lipid storage
CM trafficking	
GOTERM_CC_DIRECT	COPII vesicle coat
GOTERM_CC_DIRECT	ER to Golgi transport vesicle membrane
GOTERM_MF_DIRECT	SNARE binding
GOTERM_CC_DIRECT	SNARE complex
GOTERM_BP_DIRECT	Vesicle fusion
Eicosanoid metabolism	
UP_KEYWORDS	Leukotriene biosynthesis
GOTERM_BP_DIRECT	Leukotriene biosynthetic process
GOTERM_BP_DIRECT	Leukotriene metabolic process
GOTERM_BP_DIRECT	Prostaglandin biosynthetic process
FA modification/metabolism/transport	
GOTERM_BP_DIRECT	Fatty acid biosynthetic process
GOTERM_MF_DIRECT	3-hydroxyacyl-CoA dehydrogenase activity
INTERPRO	3-hydroxyacyl-CoA dehydrogenase, conserved site
INTERPRO	3-hydroxyacyl-CoA dehydrogenase, C-terminal
INTERPRO	3-hydroxyacyl-CoA dehydrogenase, NAD binding
GOTERM_MF_DIRECT	Acyl-CoA dehydrogenase activity
INTERPRO	Acyl-CoA dehydrogenase, conserved site
INTERPRO	Acyl-CoA dehydrogenase/oxidase
INTERPRO	Acyl-CoA dehydrogenase/oxidase C-terminal
INTERPRO	Acyl-CoA dehydrogenase/oxidase, N-terminal
GOTERM_MF_DIRECT	Acyl-CoA hydrolase activity
GOTERM_BP_DIRECT	Acyl-CoA metabolic process
INTERPRO	Acyl-CoA oxidase
PIR_SUPERFAMILY	Acyl-CoA oxidase
INTERPRO	Acyl-CoA oxidase, C-terminal
INTERPRO	Acyl-CoA oxidase/dehydrogenase, central domain
INTERPRO	AMP binding, conserved site
INTERPRO	AMP-dependent synthetase/ligase
GOTERM_MF_DIRECT	Decanoate-CoA ligase activity
INTERPRO	Domain of unknown function DUF4009
GOTERM_BP_DIRECT	Fatty acid β-oxidation
GOTERM_BP_DIRECT	Fatty acid β-oxidation using acyl-CoA dehydrogenase
GOTERM_BP_DIRECT	Fatty acid β-oxidation using acyl-CoA oxidase
KEGG_PATHWAY	Fatty acid biosynthesis
KEGG_PATHWAY	Fatty acid degradation
GOTERM_BP_DIRECT	Fatty acid elongation
GOTERM_BP_DIRECT	Fatty acid metabolic process
KEGG_PATHWAY	Fatty acid metabolism
GOTERM_BP_DIRECT	Fatty acid transport
GOTERM_MF_DIRECT	Fatty-acyl-CoA binding
GOTERM_BP_DIRECT	Fatty-acyl-CoA biosynthetic process
GOTERM_BP_DIRECT	Lipid homeostasis
GOTERM_BP_DIRECT	Long-chain fatty acid import
GOTERM_BP_DIRECT	Long-chain fatty acid metabolic process
GOTERM_MF_DIRECT	Long-chain fatty acid-CoA ligase activity
GOTERM_BP_DIRECT	Long-chain fatty-acyl-CoA biosynthetic process
GOTERM_BP_DIRECT	Long-chain fatty-acyl-CoA metabolic process
GOTERM_MF_DIRECT	Very long-chain fatty acid-CoA ligase activity
Lipid binding proteins	
INTERPRO	Acyl-CoA-binding protein, ACBP
INTERPRO	Acyl-CoA-binding protein, ACBP, conserved site
INTERPRO	Cytosolic fatty-acid binding
UP_SEQ_FEATURE	Domain: ACB
INTERPRO	Lipocalin/cytosolic fatty-acid binding protein domain
INTERPRO	Lipocalin/cytosolic fatty-acid binding protein domain
GOTERM_MF_DIRECT	Retinal binding
GOTERM_MF_DIRECT	Retinoic acid binding
GOTERM_MF_DIRECT	Retinoid binding
GOTERM_MF_DIRECT	Retinol binding
UP_KEYWORDS	Retinol binding
UP_KEYWORDS	Retinol binding
UP_KEYWORDS	Vitamin A
Lipoprotein metabolism	
INTERPRO	Apolipoprotein A1/A4/E
GOTERM_MF_DIRECT	Cholesterol binding
GOTERM_BP_DIRECT	Cholesterol efflux
GOTERM_BP_DIRECT	Cholesterol homeostasis
GOTERM_BP_DIRECT	Cholesterol metabolic process
GOTERM_MF_DIRECT	Cholesterol transporter activity
GOTERM_CC_DIRECT	Chylomicron
UP_KEYWORDS	Chylomicron
GOTERM_BP_DIRECT	Chylomicron remnant clearance
UP_KEYWORDS	HDL
GOTERM_CC_DIRECT	High-density lipoprotein particle
GOTERM_BP_DIRECT	High-density lipoprotein particle assembly
GOTERM_BP_DIRECT	High-density lipoprotein particle clearance
GOTERM_MF_DIRECT	High-density lipoprotein particle receptor binding
GOTERM_BP_DIRECT	High-density lipoprotein particle remodeling
GOTERM_CC_DIRECT	Intermediate-density lipoprotein particle
UP_KEYWORDS	LDL
SMART	LDLa
GOTERM_MF_DIRECT	Lipase inhibitor activity
UP_KEYWORDS	Lipid transport
GOTERM_BP_DIRECT	Lipid transport
GOTERM_MF_DIRECT	Lipid transporter activity
GOTERM_BP_DIRECT	Lipoprotein biosynthetic process
GOTERM_BP_DIRECT	Lipoprotein metabolic process
INTERPRO	LDL-receptor class A repeat
INTERPRO	LDL-receptor class A, conserved site
GOTERM_CC_DIRECT	LDL particle
GOTERM_BP_DIRECT	LDL particle remodeling
GOTERM_BP_DIRECT	Negative regulation of cholesterol transport
GOTERM_BP_DIRECT	Negative regulation of lipid catabolic process

Table 5. Continued

GOTERM_BP_DIRECT	Negative regulation of lipid metabolic process
GOTERM_BP_DIRECT	Negative regulation of receptor-mediated endocytosis
GOTERM_BP_DIRECT	Negative regulation of VLDL particle clearance
GOTERM_BP_DIRECT	Negative regulation of VLDL particle remodeling
GOTERM_BP_DIRECT	Neuron projection regeneration
GOTERM_MF_DIRECT	Phosphatidylcholine binding
GOTERM_MF_DIRECT	Phosphatidylcholine-sterol O-acyltransferase activator activity
GOTERM_BP_DIRECT	Phospholipid efflux
GOTERM_BP_DIRECT	Positive regulation of cholesterol esterification
GOTERM_BP_DIRECT	Positive regulation of fatty acid biosynthetic process
GOTERM_BP_DIRECT	Positive regulation of lipoprotein lipase activity
GOTERM_BP_DIRECT	Positive regulation of triglyceride catabolic process
GOTERM_BP_DIRECT	Regulation of Cdc42 protein signal transduction
GOTERM_BP_DIRECT	Regulation of intestinal cholesterol absorption
GOTERM_BP_DIRECT	Reverse cholesterol transport
GOTERM_CC_DIRECT	Spherical HDL particle
GOTERM_BP_DIRECT	Triglyceride homeostasis
GOTERM_CC_DIRECT	VLDL particle
GOTERM_BP_DIRECT	VLDL particle remodeling
UP_KEYWORDS	VLDL
TAG and PL synthesis/metabolism	
GOTERM_MF_DIRECT	1-acylglycerol-3-phosphate O-acyltransferase activity
GOTERM_BP_DIRECT	Acylglycerol catabolic process
GOTERM_MF_DIRECT	Acylglycerol lipase activity
GOTERM_BP_DIRECT	CDP-diacylglycerol biosynthetic process
GOTERM_BP_DIRECT	Ether lipid biosynthetic process
GOTERM_BP_DIRECT	Glycerolipid metabolic process
GOTERM_BP_DIRECT	Glycerophospholipid biosynthetic process
GOTERM_BP_DIRECT	Glycerophospholipid catabolic process
KEGG_PATHWAY	Glycerophospholipid metabolism
GOTERM_BP_DIRECT	GPI anchor biosynthetic process
GOTERM_MF_DIRECT	Lysophospholipase activity
GOTERM_BP_DIRECT	Phosphatidic acid biosynthetic process
UP_KEYWORDS	Phospholipid biosynthesis
GOTERM_BP_DIRECT	Phospholipid biosynthetic process
GOTERM_BP_DIRECT	Phospholipid catabolic process
GOTERM_BP_DIRECT	Phospholipid metabolic process
UP_KEYWORDS	Phospholipid metabolism
GOTERM_BP_DIRECT	Phospholipid transport
INTERPRO	Phospholipid/glycerol acyltransferase
SMART	PlsC
UP_SEQ_FEATURE	Short sequence motif: HXXXXD motif
GOTERM_BP_DIRECT	Triglyceride biosynthetic process
GOTERM_MF_DIRECT	Triglyceride lipase activity

ABCP, Acyl-CoA-binding protein; ACB, acyl-CoA-binding; AMP, Adenosine monophosphate; CDP, Cytidine Diphosphate; COPII, cytoplasmic coat protein complex II; GPI, glycosylphosphatidylinositol; HDL, high-density lipoprotein; LDL, low-density lipoprotein; LDLa, low-density lipoprotein receptor domain class A; NAD, Nicotinamide adenine dinucleotide.

Discussion

In the current study we investigated the effect of oral glucose ingestion on lipid stored in the intestine from a previous meal. We not only confirmed the ability of oral glucose to mobilize intestinal lipid stores and increase plasma CM TGs, but also expanded this observation with high-quality visualization of subcellular CLDs and lipids within the secretory pathway, as well as an examination of the intestinal proteome, to explore cellular mechanisms. Through detailed quantitative analysis of subcellular lipid depots, we showed that glucose ingestion reduced both the number and size of CLDs within enterocytes. Furthermore, our proteomic analysis of duodenal biopsy specimens showed marked differential presence of intestinal proteins in response to oral glucose compared with water, some of which may be involved in regulating the mobilization of intestinal lipid stores.

The results of the current study provide further evidence that lipid can be retained within the small intestine for many hours after fat ingestion and subsequently mobilized by a stimulus, as reviewed in the introduction. Although visualization of lipid depots in jejunal biopsy specimens was reported in a previous study,[9] our study added to the literature with examination of duodenal biopsy specimens and provided visualization of the subcellular localization of lipid droplets in the cell and in the secretory pathway. We detected the presence of abundant lipid depots, especially CLDs, within the duodenal enterocytes of subjects who ingested a high-fat meal 6 hours before the biopsy and water 1 hour before the intestinal biopsy (ie, the control study). This lipid retention in duodenal enterocytes was seen at a time that plasma TGs had almost returned to baseline, clearly showing that lipids are being retained in the intestine. Glucose ingestion acutely (within 1 hour) reduced the total amount of lipid retained in enterocytes, providing evidence of glucose-stimulated lipid mobilization. This corresponded to a spike in total plasma TGs, which was mainly owing to an increase in CM TGs. Because there was no other food intake during the study period, the high-fat liquid meal likely was the source of this TG spike. Together, these results suggest that considerable dietary lipid is retained in intestinal CLDs well into the late postprandial period, which subsequently can be mobilized and secreted within CMs. Although the results of the current study show an intracellular mechanism of CLD mobilization, lymph flow and mobilization of extracellular (eg, in lamina propria) CMs also could contribute to the overall mobilization of intestinal lipid stores. Glucose in the luminal fluid increases sympathetic activity, leading to vasodilation of the submucosal arterioles, and enhances intestinal blood flow in rodent models. Changes in vasodilation and blood flow and the potential in mediating the total response of lipid mobilization to glucose ingestion were not assessed in the current study. Increased insulin secretion after glucose ingestion also may lead to vasodilation in muscle. This may help mobilize total TG stores, but the effects of insulin on CLD mobilization are

Table 6. Lipid Metabolism Proteins Present at Relatively Different Levels in Duodenal Biopsy Specimens From Subjects Administered Glucose or Water After a High-Fat Liquid Meal

Uniprot accession	Protein name	Gene name	Fold change	*t* test *P* value	Lipid metabolism-related function
O14734	Acyl-coenzyme A thioesterase 8	ACOT8	0.2101	.0177	FA modification/ metabolism/transport
Q9NTX5	Ethylmalonyl-CoA decarboxylase	ECHDC1	0.341	.0450	FA modification/ metabolism/transport
Q9NR19	Acetyl-coenzyme A synthetase; cytoplasmic	ACSS2	0.4512	.0470	FA modification/ metabolism/transport
Q9H490	Phosphatidylinositol glycan anchor biosynthesis class U protein	PIGU	0.4799	.0487	TAG and PL synthesis/metabolism
Q15125	3-β-hydroxysteroid-Δ(8); Δ(7)-isomerase	EBP	0.4859	.0413	Cholesterol/steroid metabolism
P07108	Acyl-CoA-binding protein	DBI	0.4917	.0382	Lipid binding protein
Q9UBM7	7-dehydrocholesterol reductase	DHCR7	0.6045	.0283	Cholesterol/steroid metabolism
Q8WVX9	Fatty acyl-CoA reductase 1	FAR1	0.6231	.0223	FA modification/metabolism/transport
Q9C0D9	Ethanolaminephosphotransferase 1[a]	SELENOI	7.4638	.0005	TAG and PL synthesis/metabolism

NOTE. Proteins known to play a role in lipid metabolism were identified based on GO terms. Relative levels of proteins identified in at least 3 duodenal biopsy samples per group, or identified in at least 3 samples in 1 group and 0 samples in the other group, were compared. Proteins present at significantly different levels within the 2 treatment groups ($P < .05$, *t* test) are shown. Average fold changes of proteins in response to glucose relative to water consumption are presented. Numbers in the "Fold change" column represent how much higher (or lower if negative) the protein levels were in the glucose group compared with the water group. All of these lipid metabolism proteins were up-regulated by glucose relative to water consumption and are listed in ascending order of magnitude of fold change.
PL, phospholipid; TAG, triacylglycerol.
[a]Only identified in response to glucose.

unknown. These aspects warrant further study using animal models.

This study identifies CLDs as dynamic and regulated lipid storage depots that mediate intestinal lipid handling and CM secretion. The ability to store TGs in CLDs and mobilize this lipid pool at later times likely contributes to the efficiency of dietary fat absorption and helps prevent toxicity both locally within enterocytes as well as systemically.[4,16,17] In the enterocyte, CLDs provide a buffering depot for lipids that cannot be rapidly incorporated into CMs for secretion. Systemically, this process also may attenuate an otherwise rapid increase in postprandial lipids that could overwhelm the lipid storage and buffering capacity of adipose tissues, resulting in fatty acid spillover and lipotoxicity.[21] Furthermore, early postprandial CLD mobilization may serve as a priming function for the enterocyte's CM assembly and secretion pathway, which needs to rapidly and efficiently cope with the large influx of ingested dietary lipids during food ingestion. Quantifying lipid depots in subcellular compartments and organelles, such as detailed assessment of size distribution of chylomicrons within Golgi, may yield important information on the underlying mechanism, which was not possible with EM visualization. Together with the increase in plasma and CM TG concentrations, the results of the current study support that oral glucose functioned as a stimulus to mobilize enterocyte lipid stores for use in CM synthesis and secretion. Based on the known and well-described biology of CM assembly and secretion,[2] it is hypothesized that glucose ingestion would have initiated a sequence of events, including hydrolysis of CLD TGs, TG resynthesis in the ER membrane, CM assembly and secretion from the enterocytes, and CM transport through the lymphatics into circulation. It remains to be determined if other stimuli for intestinal lipid mobilization (eg, sham fat feeding[8] and GLP-2[19]) mobilize intestinal lipids by a similar mechanism, and whether their effects are quantitatively similar to that of oral glucose. Although glucose ingestion may stimulate the secretion of GLP-2, which mobilizes CM release, the observed effects of glucose ingestion on CLDs was unlikely owing to GLP-2 secretion. GLP-2 concentrations after 25-gram glucose ingestion is unknown and was not measured in this study because of a lack of blood samples with dipeptidyl peptidase-4 inhibitor. In healthy subjects, a standard oral glucose tolerance test (75 g D-glucose) increased plasma glucose concentrations from approximately 5 to approximately 9 mmol/L, and plasma GLP-2 concentrations from approximately 15 to 49 pmol/L.[22] Mixed meal ingestion increased plasma GLP-2 (intact, 16 ± 3 to 73 ± 10 pmol/L at 90 min), and subcutaneous injection of 400 ug GLP-2 increased intact GLP-2 to maximally 1493 ± 250 pmol/L at 45 minutes in healthy volunteers.[23] In our previous study in which GLP-2 promoted release of preformed chylomicrons, a more than 3-fold higher dose of GLP-2 was used (1500 ug),[19] which is expected to increase circulating GLP-2 even more significantly. In addition, because GLP-1 and GLP-2 are co-secreted, glucose ingestion–stimulated secretion of GLP-2 is accompanied by secretion of GLP-1, which is known to suppress CM secretion.[24] Interestingly, we found that the effects of glucose ingestion are dependent on sufficient lipid stores within the enterocyte. After prolonged fasting (10 hours after fat ingestion), which resulted in a significant reduction in intestinal CLD stores, glucose had no effect on intestinal lipid stores.

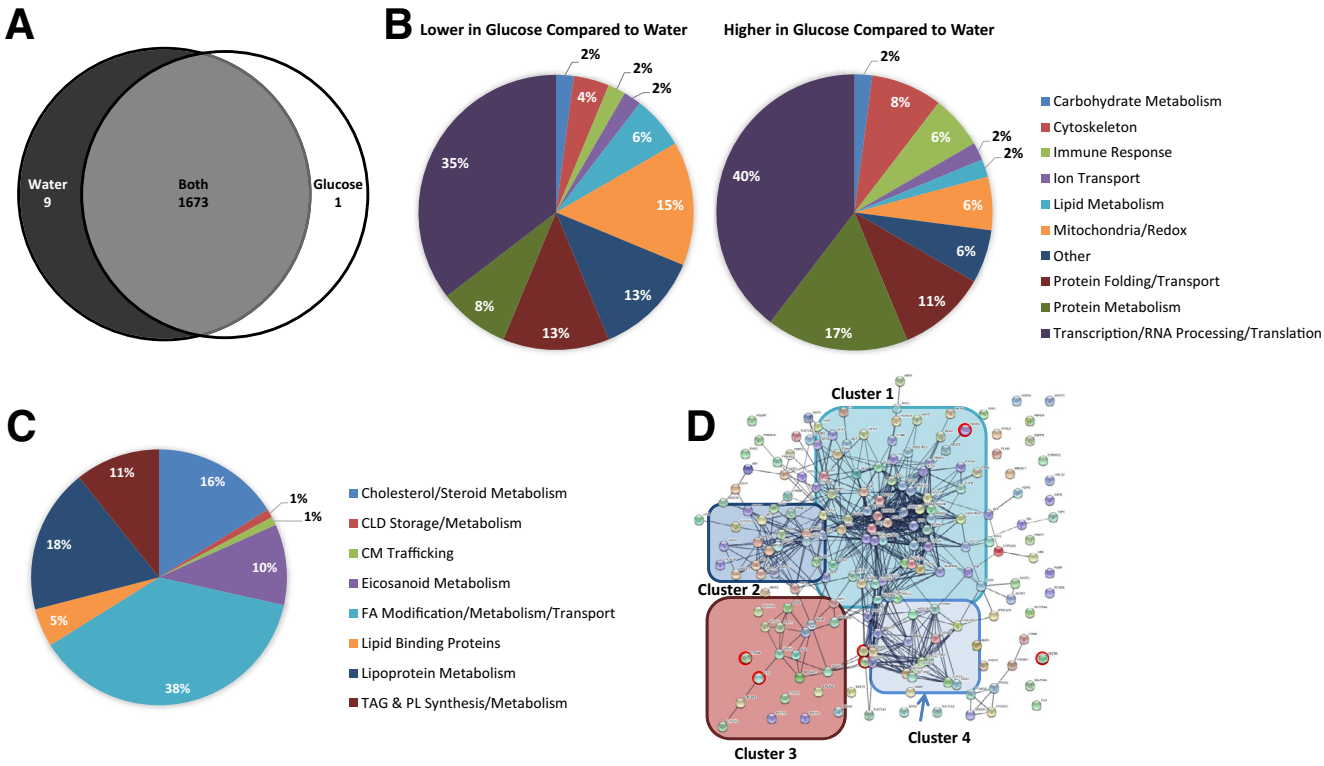

Figure 7. Proteins present in intestinal biopsy specimens from subjects administered glucose or water after an overnight fast after the consumption of a high-fat liquid meal. Duodenal biopsy specimens were collected 10 hours after lipid and 1 hour after glucose or water ingestion from patients undergoing a diagnostic endoscopy (n = 5 patients per group). (*A*) Venn diagram of proteins identified in response to glucose or water ingestion. Proteins present in at least 3 samples in 1 group and 0 samples in the other group were considered present in only 1 group. Proteins identified in at least 3 samples in 1 group and at least 1 sample in the other group were considered present in both groups. (*B*) Percentage of proteins within broad functional groups that were present at either relatively lower (48 total proteins) or relatively higher (48 total proteins) levels in response to glucose compared with water ingestion, as classified based on their biological/molecular functions. Only proteins that were identified in at least 3 samples in both groups and present at relatively different levels ($P < .05$, *t* test), or at least 3 samples in 1 group and 0 samples in the other group, were included in this classification. A Database for Annotation, Visualization, and Integrated Discovery search of the 1683 identified proteins resulted in the identification of 186 proteins with GO terms related to lipid metabolism. (*C*) Percentage of the 186 lipid metabolism-related proteins involved in more specific lipid-related functions. (*D*) String analysis of the 186 lipid metabolism-related proteins. The thickness of the *line* represents the strength of evidence of a structural/functional relationship between 2 proteins. Cluster 1 is enriched in proteins involved in FA modification/metabolism/transport, cluster 2 is enriched in proteins involved in lipoprotein metabolism, cluster 3 is enriched in proteins involved in TG and phospholipid (PL) synthesis and metabolism, and cluster 4 is enriched in proteins involved in cholesterol/steroid metabolism. Proteins that were present at relatively different levels ($P < .05$, *t* test) in response to glucose compared with water ingestion are *circled in red*.

To gain further insight into proteins potentially regulating the observed glucose-stimulated lipid mobilization within the small intestine, we performed a comparative proteomic analysis of the duodenal biopsy specimens in response to glucose compared with water ingestion. Previous studies have used both untargeted and targeted approaches to identify duodenal proteins in insulin-resistant compared with insulin-sensitive individuals, but these duodenal tissue samples were collected in the fasted state.[25,26] Although validation of the presence of the identified proteins within the small intestine by additional methods is needed, the present study provides us with candidate proteins that are present in the duodenum in response to dietary fat and glucose ingestion. This study also identified potential glucose-regulated proteins within the duodenum, some of which also may be involved in regulating glucose-stimulated mobilization of lipids from the small intestine. In the current study we initially used a *P* value less than .05 as the cut-off value to identify proteins differentially present between treatment groups. After Bonferroni correction for multiple comparisons, a few proteins were still present at significantly different levels between the groups. It is important to note that the Bonferroni correction is a stringent correction factor that minimizes false-positive results, but it also increases false-negative results. Therefore, although this correction factor helps prioritize candidate proteins for further investigation, the current proteomic analysis is a hypothesis-generating experiment, and it is therefore also important to not completely disregard the proteins that were no

Table 7. Proteins Present at Relatively Different Levels in Duodenal Biopsy Specimens From Subjects Administered Glucose or Water After an Overnight Fast After the Consumption of a High-Fat Liquid Meal

Uniprot accession	Protein name	Gene name	Fold change	*t* test *P* value	Function
P02760	Protein AMBP[a]	AMBP	-10.9586	2.33E-05	Protein metabolism
P35613	Basigin[a]	BSG	-7.4781	1.28E-05	Other (extracellular matrix organization)
P42025	β-centractin[a]	ACTR1B	-6.6073	.0003	Cytoskeleton
Q96GA7	Serine dehydratase-like[a]	SDSL	-6.4238	4.13E-05	Protein metabolism
Q9NP81	Serine-tRNA ligase; mitochondrial[a]	SARS2	-6.4093	.0001	Transcription/RNA processing/translation
Q07837	Neutral and basic amino acid transport protein rBAT[a]	SLC3A1	-5.9686	.0001	Protein folding/transport
Q9NW15	Anoctamin-10[a]	ANO10	-5.8317	6.88E-13	Ion transport
P33897	ATP-binding cassette subfamily D member 1[a]	ABCD1	-5.296	.0011	Lipid metabolism
Q9Y320	Thioredoxin-related transmembrane protein 2[a]	TMX2	-4.7109	.0055	Mitochondria/redox
P62899	60S ribosomal protein L31	RPL31	-1.4463	.0016	Transcription/RNA processing/translation
P26583	High-mobility group protein B2	HMGB2	-1.3698	.0205	Transcription/RNA processing/translation
P62841	40S ribosomal protein S15	RPS15	-1.339	.0217	Transcription/RNA processing/translation
O43895	Xaa-Pro aminopeptidase 2	XPNPEP2	-1.2009	.0161	Protein metabolism
Q00688	Peptidyl-prolyl cis-trans isomerase FKBP3	FKBP3	-1.1226	.0486	Protein folding/transport
P62424	60S ribosomal protein L7a	RPL7A	-1.0994	.0165	Transcription/RNA processing/translation
P99999	Cytochrome c	CYCS	-1.0634	.0237	Mitochondria/redox
P14927	Cytochrome b-c1 complex subunit 7	UQCRB	-0.9939	.0352	Mitochondria/redox
O43181	NADH dehydrogenase (ubiquinone) iron-sulfur protein 4; mitochondrial	NDUFS4	-0.9391	.0220	Mitochondria/redox
P46783	40S ribosomal protein S10	RPS10	-0.8004	.0412	Transcription/RNA processing/translation
Q9UNX3	60S ribosomal protein L26-like 1	RPL26L1	-0.795	.0441	Transcription/RNA processing/translation
P62241	40S ribosomal protein S8	RPS8	-0.7606	.0362	Transcription/RNA processing/translation
Q00013	55-kilodalton erythrocyte membrane protein	MPP1	-0.6858	.0323	Immune response
Q9Y3U8	60S ribosomal protein L36	RPL36	-0.6824	.0149	Transcription/RNA processing/translation
P04792	Heat shock protein β-1	HSPB1	-0.6317	.0415	Protein folding/transport
P20674	Cytochrome c oxidase subunit 5A; mitochondrial	COX5A	-0.6209	.0430	Mitochondria/redox
Q9BXW7	Haloacid dehalogenase-like hydrolase domain-containing 5	HDHD5	-0.5832	.0196	Lipid metabolism
P62081	40S ribosomal protein S7	RPS7	-0.5799	.0368	Transcription/RNA processing/translation
Q92520	Protein FAM3C	FAM3C	-0.5691	.0467	Other (cytokine activity)
Q86VU5	Catechol O-methyltransferase domain-containing protein 1	COMTD1	-0.5488	.0242	Other (putative O-methyltransferase)
Q15233	Non-POU domain-containing octamer-binding protein	NONO	-0.5382	.0131	Transcription/RNA processing/translation
P08708	40S ribosomal protein S17	RPS17	-0.5285	.0429	Transcription/RNA processing/translation
Q5SSJ5	Heterochromatin protein 1-binding protein 3	HP1BP3	-0.5232	.0430	Transcription/RNA processing/translation
P26232	Catenin α-2	CTNNA2	-0.5041	.0231	Cytoskeleton
O60825	6-phosphofructo-2-kinase/fructose-2;6-bisphosphatase 2	PFKFB2	-0.4706	.0010	Carbohydrate metabolism

Table 7. Continued

Uniprot accession	Protein name	Gene name	Fold change	*t* test *P* value	Function
Q9BPW8	Protein NipSnap homolog 1	NIPSNAP1	-0.4247	.0273	Mitochondria/redox
Q9BUJ2	Heterogeneous nuclear ribonucleoprotein U-like protein 1	HNRNPUL1	-0.4204	.0322	Transcription/RNA processing/translation
P51148	Ras-related protein Rab-5C	RAB5C	-0.4166	.0228	Protein folding/transport
A0AV96	RNA-binding protein 47	RBM47	-0.4047	.0211	Other (RNA binding)
P26373	60S ribosomal protein L13	RPL13	-0.3879	.0418	Transcription/RNA processing/translation
Q9Y6N9	Harmonin	USH1C	-0.3863	.0445	Other (brush-border assembly, regulation of microvillus length)
Q5IFJ7	60S ribosomal protein L9	RPL9	-0.3797	.0444	Transcription/RNA processing/translation
P36543	V-type proton ATPase subunit E 1	ATP6V1E1	-0.3609	.0298	Mitochondria/redox
P15880	40S ribosomal protein S2	RPS2	-0.313	.0103	Transcription/RNA processing/translation
Q00169	Phosphatidylinositol transfer protein α isoform	PITPNA	-0.2974	.0315	Lipid metabolism
Q9Y4W6	AFG3-like protein 2	AFG3L2	-0.2882	.0427	Protein metabolism
Q9UBQ0	Vacuolar protein sorting-associated protein 29	VPS29	-0.283	.0334	Protein folding/transport
Q13232	Nucleoside diphosphate kinase 3	NME3	-0.2655	.0405	Other (nucleotide triphosphate synthesis)
P61106	Ras-related protein Rab-14	RAB14	-0.2269	.0176	Protein folding/transport
Q8NEV1	Casein kinase II subunit α 3	CSNK2A3	0.1846	.0033	Protein metabolism
Q9BPX5	Actin-related protein 2/3 complex subunit 5-like protein	ARPC5L	0.2192	.0094	Transcription/RNA processing/translation
Q7L5N1	COP9 signalosome complex subunit 6	COPS6	0.2227	.0237	Protein metabolism
O60313	Dynamin-like 120-kilodalton protein; mitochondrial	OPA1	0.2682	.0189	Mitochondria/redox
Q15029	116-kilodalton U5 small nuclear ribonucleoprotein component	EFTUD2	0.2702	.0022	Transcription/RNA processing/translation
Q92841	Probable ATP-dependent RNA helicase DDX17	DDX17	0.2774	.0277	Transcription/RNA processing/translation
Q9Y265	RuvB-like 1	RUVBL1	0.2863	.0143	Transcription/RNA processing/translation
Q08211	ATP-dependent RNA helicase A	DHX9	0.2969	.0021	Transcription/RNA processing/translation
P56192	Methionine-tRNA ligase; cytoplasmic	MARS	0.2985	.0005	Transcription/RNA processing/translation
O00303	Eukaryotic translation initiation factor 3 subunit F	EIF3F	0.3017	.0358	Transcription/RNA processing/translation
P50990	T-complex protein 1 subunit theta	CCT8	0.3103	.0462	Protein folding/transport
Q13363	C-terminal-binding protein 1	CTBP1	0.3117	.0193	Transcription/RNA processing/translation
O76094	Signal recognition particle subunit SRP72	SRP72	0.317	.0088	Transcription/RNA processing/translation
P50851	Lipopolysaccharide-responsive and beige-like anchor protein	LRBA	0.3239	.0462	Immune response
Q13409	Cytoplasmic dynein 1 intermediate chain 2	DYNC1I2	0.3304	.0080	Cytoskeleton
Q6P2Q9	Pre–messenger RNA-processing-splicing factor 8	PRPF8	0.3428	.0263	Transcription/RNA processing/translation
P46940	Ras GTPase-activating-like protein IQGAP1	IQGAP1	0.3464	.0427	Other (cellular response to calcium and growth factor stimuli)
O95782	AP-2 complex subunit α-1	AP2A1	0.3545	.0240	Protein folding/transport
P17987	T-complex protein 1 subunit α	TCP1	0.3631	.0078	Protein folding/transport
Q14152	Eukaryotic translation initiation factor 3 subunit A	EIF3A	0.3778	.0231	Transcription/RNA processing/translation
O95394	Phosphoacetylglucosamine mutase	PGM3	0.3795	.0164	Carbohydrate metabolism

Table 7. Continued

Uniprot accession	Protein name	Gene name	Fold change	*t* test *P* value	Function
O43143	Pre–messenger RNA-splicing factor ATP-dependent RNA helicase DHX15	DHX15	0.3864	.0448	Transcription/RNA processing/translation
Q9P2J5	Leucine-tRNA ligase; cytoplasmic	LARS	0.3966	.0183	Transcription/RNA processing/translation
P13010	X-ray repair cross-complementing protein 5	XRCC5	0.4032	.0284	Transcription/RNA processing/translation
O75643	U5 small nuclear ribonucleoprotein 200-kilodalton helicase	SNRNP200	0.404	.0136	Transcription/RNA processing/translation
Q53EL6	Programmed cell death protein 4	PDCD4	0.4079	.0175	Transcription/RNA processing/translation
Q8N163	Cell cycle and apoptosis regulator protein 2	CCAR2	0.4108	.0094	Transcription/RNA processing/translation
Q15008	26S proteasome non-ATPase regulatory subunit 6	PSMD6	0.4158	.0475	Protein metabolism
P00325	Alcohol dehydrogenase 1B	ADH1B	0.427	.0394	Mitochondria/redox
P07478	Trypsin-2	PRSS2	0.4359	.0328	Protein metabolism
Q9Y262	Eukaryotic translation initiation factor 3 subunit L	EIF3L	0.4529	.0493	Transcription/RNA processing/translation
Q93009	Ubiquitin carboxyl-terminal hydrolase 7	USP7	0.455	.0294	Protein metabolism
Q86VP6	Cullin-associated NEDD8-dissociated protein 1	CAND1	0.4561	.0490	Protein metabolism
O00410	Importin-5	IPO5	0.4754	.0232	Protein folding/transport
Q15393	Splicing factor 3B subunit 3	SF3B3	0.4946	.0349	Transcription/RNA processing/translation
P07437	Tubulin β chain	TUBB	0.5145	.0031	Cytoskeleton
P55011	Solute carrier family 12 member 2	SLC12A2	0.5237	.0405	Ion transport
Q14974	Importin subunit β-1	KPNB1	0.5474	.0326	Protein folding/transport
P0DOX7	Immunoglobulin κ light chain		0.5546	.0356	Immune response
P68363	Tubulin α-1B chain	TUBA1B	0.5982	.0022	Cytoskeleton
P55786	Puromycin-sensitive aminopeptidase	NPEPPS	0.5983	.0495	Protein metabolism
P11766	Alcohol dehydrogenase class-3	ADH5	0.5992	.0360	Mitochondria/redox
P05451	Lithostathine-1-α	REG1A	0.6105	.0107	Other (positive regulator of cell proliferation, carbohydrate binding)
Q9BUF5	Tubulin β-6 chain	TUBB6	0.6265	.0332	Cytoskeleton
P01619	Immunoglobulin κ variable 3–20	IGKV3-20	1.0274	.0314	Immune response
O00534	von Willebrand factor A domain-containing protein 5A	VWA5A	1.1874	.0346	Other (may act as tumor suppressor)
P08311	Cathepsin G	CTSG	1.8843	.0438	Protein metabolism
Q8IV08	Phospholipase D3[b]	PLD3	5.5249	1.31E-08	Lipid metabolism

NOTE. Duodenal biopsy samples were collected 10 hours after lipid and 1 hour after glucose or water ingestion from patients undergoing a diagnostic endoscopy (n = 5 patients per group). Proteins that were identified in at least 3 samples in both groups and present at relatively different levels ($P < .05$, *t* test), or at least 3 samples in 1 group and 0 samples in the other group, are shown. Average fold changes of proteins in response to glucose relative to water consumption are presented. Numbers in the "Fold change" column represent how much higher (or lower if negative) the protein levels were in the glucose group compared with the water group.
AMBP, alpha-1-microglobulin/bikunin precursor; AP-2, adaptor protein complex 2; ATP, adenosine triphosphate; ATPase, adenosine triphosphatase; GTPase, guanosine triphosphatase; rBAT, neutral and basic amino acid transport protein; redox, reduction-oxidation; tRNA, transfer ribonucleic acid.
[a]Only identified in response to water.
[b]Only identified in response to glucose.

Table 8. GO Terms Associated With Lipid Metabolism-Related Proteins Present in Duodenal Biopsy Specimens 10 Hours After a High-Fat Liquid Meal

Cholesterol/steroid metabolism	
UP_KEYWORDS	Cholesterol biosynthesis
GOTERM_BP_DIRECT	Cholesterol biosynthetic process
UP_KEYWORDS	Cholesterol metabolism
GOTERM_BP_DIRECT	Isoprenoid biosynthetic process
UP_KEYWORDS	Steroid biosynthesis
KEGG_PATHWAY	Steroid hormone biosynthesis
GOTERM_BP_DIRECT	Steroid metabolic process
UP_KEYWORDS	Steroid metabolism
UP_KEYWORDS	Sterol biosynthesis
GOTERM_MF_DIRECT	Sterol esterase activity
UP_KEYWORDS	Sterol metabolism
CLD storage/metabolism	
GOTERM_CC_DIRECT	Lipid droplet
GOTERM_BP_DIRECT	Lipid storage
CM trafficking	
GOTERM_CC_DIRECT	ER to Golgi transport vesicle membrane
Eicosanoid metabolism	
GOTERM_MF_DIRECT	Arachidonic acid epoxygenase activity
KEGG_PATHWAY	Arachidonic acid metabolism
GOTERM_BP_DIRECT	Cyclooxygenase pathway
GOTERM_BP_DIRECT	Epoxygenase P450 pathway
GOTERM_BP_DIRECT	Leukotriene metabolic process
UP_KEYWORDS	Prostaglandin biosynthesis
GOTERM_BP_DIRECT	Prostaglandin biosynthetic process
UP_KEYWORDS	Prostaglandin metabolism
GOTERM_MF_DIRECT	Steroid hydroxylase activity
FA modification/metabolism/transport	
GOTERM_MF_DIRECT	Acyl-CoA dehydrogenase activity
INTERPRO	Acyl-CoA dehydrogenase, conserved site
INTERPRO	Acyl-CoA dehydrogenase/oxidase
INTERPRO	Acyl-CoA dehydrogenase/oxidase, C-terminal
INTERPRO	Acyl-CoA dehydrogenase/oxidase, N-terminal
GOTERM_MF_DIRECT	Acyl-CoA hydrolase activity
GOTERM_BP_DIRECT	Acyl-CoA metabolic process
INTERPRO	Acyl-CoA oxidase/dehydrogenase, central domain
INTERPRO	Acyltransferase ChoActase/COT/CPT
INTERPRO	AMP binding, conserved site
INTERPRO	AMP-dependent synthetase/ligase
UP_SEQ_FEATURE	Binding site: carnitine
GOTERM_MF_DIRECT	Decanoate-CoA ligase activity
INTERPRO	Domain of unknown function DUF4009
GOTERM_BP_DIRECT	Fatty acid α-oxidation
GOTERM_BP_DIRECT	Fatty acid β-oxidation
GOTERM_BP_DIRECT	Fatty acid β-oxidation using acyl-CoA dehydrogenase
UP_KEYWORDS	Fatty acid biosynthesis
KEGG_PATHWAY	Fatty acid biosynthesis
KEGG_PATHWAY	Fatty acid degradation
UP_KEYWORDS	Fatty acid metabolism
KEGG_PATHWAY	Fatty acid metabolism
GOTERM_MF_DIRECT	Flavin adenine dinucleotide binding
GOTERM_MF_DIRECT	Hydroxyacyl-CoA dehydrogenase activity
GOTERM_BP_DIRECT	Lipid homeostasis
GOTERM_BP_DIRECT	Long-chain fatty acid import
GOTERM_BP_DIRECT	Long-chain fatty acid metabolic process
GOTERM_MF_DIRECT	Long-chain fatty acid–CoA ligase activity
GOTERM_BP_DIRECT	Negative regulation of fatty acid metabolic process
GOTERM_MF_DIRECT	Oxidoreductase activity, acting on the CH-CH group of donors
GOTERM_MF_DIRECT	Oxidoreductase activity, acting on the CH-CH group of donors, with a flavin as acceptor
GOTERM_MF_DIRECT	Palmitoyl-CoA hydrolase activity
UP_SEQ_FEATURE	Region of interest: coenzyme A binding
GOTERM_MF_DIRECT	Transferase activity, transferring acyl groups
GOTERM_MF_DIRECT	Very-long-chain fatty acid–CoA ligase activity
Lipid binding proteins	
INTERPRO	Acyl-CoA binding protein, ACBP
INTERPRO	Acyl-CoA binding protein, ACBP, conserved site
INTERPRO	Cytosolic fatty acid binding
UP_SEQ_FEATURE	Domain: ACB
GOTERM_MF_DIRECT	Fatty-acyl-CoA binding
INTERPRO	Lipocalin/cytosolic fatty acid binding protein domain
GOTERM_MF_DIRECT	Retinoic acid binding
Lipoprotein metabolism	
INTERPRO	Apolipoprotein A1/A4/E
GOTERM_MF_DIRECT	Cholesterol binding
GOTERM_BP_DIRECT	Cholesterol efflux
GOTERM_BP_DIRECT	Cholesterol homeostasis
GOTERM_BP_DIRECT	Cholesterol metabolic process
GOTERM_MF_DIRECT	Cholesterol transporter activity
GOTERM_CC_DIRECT	Chylomicron
UP_KEYWORDS	Chylomicron
GOTERM_BP_DIRECT	Chylomicron remnant clearance
UP_KEYWORDS	High-density lipoprotein
GOTERM_CC_DIRECT	High-density lipoprotein particle
GOTERM_BP_DIRECT	High-density lipoprotein particle assembly
GOTERM_BP_DIRECT	High-density lipoprotein particle clearance
GOTERM_MF_DIRECT	High-density lipoprotein particle receptor binding
GOTERM_BP_DIRECT	High-density lipoprotein particle remodeling
GOTERM_CC_DIRECT	Intermediate-density lipoprotein particle
GOTERM_MF_DIRECT	Lipase inhibitor activity
UP_KEYWORDS	Lipid transport
GOTERM_BP_DIRECT	Lipid transport
GOTERM_MF_DIRECT	Lipid transporter activity
GOTERM_BP_DIRECT	Lipoprotein biosynthetic process
GOTERM_BP_DIRECT	Lipoprotein metabolic process
GOTERM_CC_DIRECT	Low-density lipoprotein particle
GOTERM_BP_DIRECT	Low-density lipoprotein particle remodeling
GOTERM_BP_DIRECT	Negative regulation of cholesterol transport
GOTERM_BP_DIRECT	Negative regulation of lipid catabolic process
GOTERM_BP_DIRECT	Negative regulation of lipid metabolic process
GOTERM_BP_DIRECT	Negative regulation of receptor-mediated endocytosis
GOTERM_BP_DIRECT	Negative regulation of VLDL particle clearance

Table 8. Continued

GOTERM_BP_DIRECT	Negative regulation of VLDL particle remodeling
GOTERM_MF_DIRECT	Phosphatidylcholine binding
GOTERM_MF_DIRECT	Phosphatidylcholine-sterol O-acyltransferase activator activity
GOTERM_BP_DIRECT	Phospholipid efflux
GOTERM_BP_DIRECT	Positive regulation of cholesterol esterification
GOTERM_BP_DIRECT	Positive regulation of fatty acid biosynthetic process
GOTERM_BP_DIRECT	Positive regulation of lipoprotein lipase activity
GOTERM_BP_DIRECT	Positive regulation of triglyceride catabolic process
GOTERM_BP_DIRECT	Regulation of Cdc42 protein signal transduction
GOTERM_BP_DIRECT	Regulation of intestinal cholesterol absorption
GOTERM_BP_DIRECT	Reverse cholesterol transport
GOTERM_CC_DIRECT	Spherical high-density lipoprotein particle
GOTERM_BP_DIRECT	Triglyceride catabolic process
GOTERM_BP_DIRECT	Triglyceride homeostasis
GOTERM_CC_DIRECT	VLDL particle
GOTERM_BP_DIRECT	VLDL particle remodeling
UP_KEYWORDS	VLDL
TAG and PL synthesis/metabolism	
GOTERM_MF_DIRECT	1-Acylglycerol-3-phosphate O-acyltransferase activity
GOTERM_MF_DIRECT	1-Acylglycerol-3-phosphate O-acyltransferase activity
GOTERM_BP_DIRECT	Acylglycerol catabolic process
GOTERM_BP_DIRECT	CDP-diacylglycerol biosynthetic process
GOTERM_BP_DIRECT	CDP-diacylglycerol biosynthetic process
GOTERM_BP_DIRECT	Glycerophospholipid biosynthetic process
	Glycerophospholipid biosynthetic process
GOTERM_BP_DIRECT	Glycerophospholipid catabolic process
KEGG_PATHWAY	Glycerophospholipid metabolism
GOTERM_BP_DIRECT	Phosphatidic acid biosynthetic process
UP_KEYWORDS	Phospholipid biosynthesis
GOTERM_BP_DIRECT	Phospholipid biosynthetic process
UP_KEYWORDS	Phospholipid metabolism
INTERPRO	Phospholipid/glycerol acyltransferase
GOTERM_BP_DIRECT	Triglyceride biosynthetic process
GOTERM_BP_DIRECT	Triglyceride lipase activity

ACBP, acyl-CoA-binding protein; AMP, adenosine monophosphate; CDP, cytidine diphosphate; COT/CPT, carnitine octanoyltransferase/carnitine palmitoyltransferase.

longer present at significantly different levels after this correction.

To identify proteins potentially involved in regulating glucose-stimulated lipid mobilization from the small intestine, we performed a targeted search of our proteomics data to identify proteins with known roles in intestinal lipid/lipoprotein metabolism and transport. The results suggest differential regulation of proteins involved in fatty acid metabolism, cholesterol synthesis, and lipid binding. Little is known about the particular roles of these proteins within the small intestine specifically. However, acyl-coenzyme A binding protein previously was shown to be present at high levels in mouse intestinal epithelium and to co-localize with fatty acid binding protein 2 (intestinal fatty-acid binding protein).[27] Fatty acid binding protein 2 also was identified in the current study but was present at similar levels in both treatments. Interestingly, we found that ethanolaminephosphotransferase 1 was relatively up-regulated by glucose ingestion. This protein is involved in the synthesis of phosphatidylethanolamine.[28] Mutations in several enzymes involved in phospholipid synthesis are associated with diseases including fatty liver, lipodystrophy, and obesity.[29] In addition, altering the phospholipid composition of CLDs, CMs, and the ER all have the potential to impact lipid storage and secretion, such as in phospholipid remodeling protein lysophosphatidylcholine acyltransferase-3 deficiency.[30] Therefore, it is possible that higher levels of ethanolaminephosphotransferase 1 in the intestine in response to glucose has an impact on membrane composition of the ER and/or CMs that ultimately promotes CM secretion. Validation of the presence and localization of these proteins within the small intestine, which was not possible owing to a lack of suitable samples in this study, is required in future studies, but their initial identification and differential presence in the 2 treatment groups suggests there may be a general increase in intestinal lipid metabolism in response to glucose consumption. Furthermore, the differentially present lipid metabolism-related proteins identified in biopsy specimens after prolonged (10 hours) fasting were not the same as those identified in the shorter (6 hour) fasting study, but they were involved in similar processes. This suggests that glucose may exert different regulatory effects depending on dietary status (ie, when the last meal was consumed).

Interestingly, we did not see differences in the levels of several proteins with established roles in CM synthesis and secretion or CLD metabolism between treatments. We identified both perilipin 2 and perilipin 3, which play roles in regulating CLD storage,[31] but these proteins were present at similar levels in both treatment groups. In addition, we only identified 1 of the 4 enzymes involved in cytoplasmic TG lipolysis, monoacylglycerol lipase, in the current study, and it was not differentially present in response to glucose compared with water ingestion. This is consistent, however, with the lack of identification of any cytoplasmic lipases other than monoacylglycerol lipase within duodenal tissues collected from fasted insulin-sensitive or insulin-resistant individuals.[26] It is possible that these proteins are present at levels below the mass spectrometry detection limit, and/or that other enzymes or pathways play more of a role in TG mobilization from enterocytes under the conditions of the current study. In fact, we identified lysosomal acid lipase, which hydrolyzes TGs within the lysosome during lipophagy,[32] at similar levels in both treatment groups, along with several other lipases. We also identified key proteins involved in CM synthesis and trafficking (apolipoprotein B, microsomal triglyceride transfer protein, secretion associated ras related GTPase 1B), but again did not see

Table 9. Lipid Metabolism Proteins Present at Relatively Different Levels in Duodenal Biopsy Specimens in Response to Glucose or Water Consumption After an Overnight Fast After the Consumption of a High-Fat Liquid Meal

Uniprot accession	Protein name	Gene name	Fold change	*t* test *P* value	Lipid metabolism-related function
P33897	ATP binding cassette subfamily D member 1[a]	ABCD1	-5.296	.00108	FA modification/ metabolism/transport
Q9BXW7	Haloacid dehalogenase-like hydrolase domain-containing 5	HDHD5	-0.5832	.0196	TAG and PL synthesis/metabolism
Q00169	Phosphatidylinositol transfer protein α isoform	PITPNA	-0.2974	.0315	Lipoprotein metabolism
P00325	Alcohol dehydrogenase 1B	ADH1B	0.427	.0394	FA modification/ metabolism/transport
P11766	Alcohol dehydrogenase class-3	ADH5	0.5992	.0360	FA modification/ metabolism/transport
Q8IV08	Phospholipase D3[b]	PLD3	5.5249	1.31E-08	TAG and PL synthesis/ metabolism

NOTE. Duodenal biopsy samples were collected 10 hours after lipid and 1 hour after glucose or water ingestion from patients undergoing a diagnostic endoscopy (n = 5 patients per group). Lipid metabolism-related proteins were identified based on GO terms, and relative levels of proteins identified in at least 3 duodenal biopsy samples per group, or identified in at least 3 samples in 1 group and 0 samples in the other group, were compared. Numbers in the "Fold change" column represent how much higher (or lower if negative) the protein levels were in the glucose group compared with the water group. Proteins present at significantly different levels within the 2 treatment groups ($P < .05$, *t* test) are shown.
ATP, adenosine triphosphate; PL, phospholipid, TAG, triacylglycerol.
[a]Only identified in response to water.
[b]Only identified in response to glucose.

differences in their protein levels in response to glucose compared with water ingestion. However, it still is possible that glucose ingestion alters the activities (eg, through phosphorylation) or subcellular localization of proteins involved in CM synthesis and CLD metabolism, which requires further investigation in future studies.

To examine whether proteins without known roles in lipid metabolism are involved in the observed glucose-stimulated mobilization from the small intestine, we also examined non–lipid-related proteins. This analysis showed that glucose down-regulated syntaxin-binding protein 5. This protein has been shown to be a negative regulator of soluble *N*-ethylmaleimide-sensitive factor attachment protein receptor (SNARE) protein assembly required for insulin exocytosis in β cells. In addition, glucose has been shown to inhibit syntaxin-binding protein 5 and induce its degradation in these cells to promote insulin secretion.[33] Furthermore, it regulates vesicle exocytosis in other cell types, including platelets and endothelial cells.[34] In enterocytes, SNARE complex is required for prechylomicron transport vesicle intracellular transport during chylomicron synthesis and secretion. After budding from the ER, prechylomicron transport vesicles are directed by vesicle SNARE toward the Golgi. Vesicle associated membrane protein 7 of the vesicle SNARE joins with syntaxin-5, rbet1, and vti1a of the target SNARE to form the SNARE complex, which facilitates docking and fusion of prechylomicron transport vesicle with the Golgi membrane.[35] The roles of syntaxin-binding protein 5 in enterocytes are not elucidated, but our data suggest that glucose negatively regulates this protein in enterocytes, and that this regulation may have an impact on intestinal lipid mobilization. Another protein that draws attention is epimerase family protein SDR39U1, which was up-regulated by glucose. This protein is expressed in small intestine, including the duodenum.[36] It belongs to a family of enzymes involved in the metabolism of a large variety of compounds, including steroid hormones, prostaglandins, retinoids, lipids, and xenobiotics.[37] Genetic defects in SDR genes underlie several inherited metabolic diseases.[38] Further investigation into the intestine-specific functions of these proteins would be beneficial because of their possible involvement in glucose-stimulated lipid mobilization from the intestine.

Conclusions

Here, we present evidence from both in vivo lipid responses and intestinal biopsy specimens that support a role of glucose ingestion in mobilizing lipid stores from the human intestine. Glucose ingestion mobilizes enterocyte CLDs to provide substrate for CM synthesis and secretion, likely involving multiple molecular players. Although the precise mechanisms by which intestinal lipid stores are mobilized remain unknown, the current study has highlighted candidate proteins and pathways that may regulate this process and can inform future studies investigating the regulation of this process. An increased understanding of the regulation of intestinal lipid storage and mobilization may help provide novel dietary guidance for lowering blood TG levels and identify novel therapeutic targets for treatment of hypertriglyceridemia to reduce cardiovascular disease risk.

Materials and Methods

Aim 1

Subjects. Six healthy men were recruited through advertisement in a local newspaper. Subjects were in good health, with no known medical conditions, and were not taking any medication. The study protocol was approved by the Research Ethics Board at the University Health Network,

University of Toronto. All participants provided written informed consent.

Study protocol. Each subject was studied on 2 occasions, 4–6 weeks apart, in random order. On each occasion, subjects were admitted to the Metabolic Test Centre at the Toronto General Hospital after an overnight fast. An indwelling catheter was inserted into a superficial arm vein for blood sampling. At 7 AM (referred to as t = 0), subjects ingested a 100-mL high-fat liquid meal (Calogen; Nutricia Advanced Medical Nutrition, Wiltshire, UK). Each 100 mL of the liquid meal contains 450 kcal energy, 50 g fat (5.3 g saturated fat, 30.4 g monounsaturated fat, 14.3 g polyunsaturated fat), 0 g protein, and 0.1 g carbohydrate. Five hours later (t = 5 h), subjects ingested a glucose solution (50%, 50 mL) in 1 arm of the study and 50 mL water in the other arm, 4–6 weeks apart. Blood samples were drawn at baseline and at regular intervals until the end of the study (t = 8 h).

Laboratory analysis. TRL was first isolated as previously described.[24] CM and VLDL-sized particles were isolated further from TRL, according to a previously described method with modifications.[19,39] TRL fractions (1 mL) were transferred to a 6-mL centrifuge tube on ice, carefully overlaid with 1.006 g/mL density NaBr solution, and centrifuged at 13,500 rpm for 30 minutes at 12°C using a Ti50.4 rotor. Clear separation was visible between the top and bottom fractions. The top 0.5 mL was collected as CM by tube slicing, whereas the bottom fraction was collected as VLDL-sized lipoproteins. Plasma glucose was measured at the bedside with a glucose analyzer (Analox Instruments, Stourbridge, UK). TG in plasma and lipoprotein fractions were measured with a commercial kit (Roche Diagnostics, Indianapolis, IN). Plasma insulin was measured with a human insulin radioimmunoassay kit (Millipore, Burlington, MA).

Aim 2

Subjects. Twenty-four individuals undergoing diagnostic gastroduodenoscopy for gastrointestinal symptoms were recruited after obtaining informed consent. Subjects were referred for endoscopy after complaints of heartburn, dyspepsia, bloating, abdominal pain, nausea without vomiting, reflux, gas, and regurgitation. Participants had no known duodenal pathology and were observed to have normal duodenal mucosa by visual inspection during the endoscopy. The study protocol was approved by the Human Research Ethics Board of the University Health Network, University of Toronto. All participants provided written informed consent.

Study protocol. After providing informed consent, participants were block-randomized to receive either oral glucose or water treatment. At 7 AM after an overnight fast (referred to as t = 0), subjects ingested a 100-mL high-fat liquid meal containing 50 g of fat (Calogen; Nutricia Advanced Medical Nutrition). Five hours later (t = 5 h), subjects ingested either a glucose solution (50%, 50 mL) or 50 mL water. One hour after ingesting either glucose or water (t = 6 h), duodenal biopsy samples were obtained during an endoscopy. Although quantitatively jejunum is responsible for the majority of lipid absorption, active absorption also occurs in duodenum[40] and obtaining biopsy specimens from the duodenum as compared with jejunum is more technically feasible and was acceptable to our human ethics review committee. Samples were snap-frozen in dry ice and stored at -80°C for later proteomic analysis or preserved in 2.5% glutaraldehyde in 0.1 mol/L sodium cacodylate (pH 7.4) and stored at 4°C for electron microscopy.

Delayed fasting. To further examine the time course of fat retention in the intestine and its subsequent mobilization by oral glucose, duodenal biopsy specimens were taken from an additional 10 individuals. These individuals were randomly assigned to ingest glucose or water 9 hours after ingestion of the high-fat liquid meal, which was administered at 10 PM the night before undergoing the gastroduodenoscopy. The study protocol was otherwise identical to that described earlier for aim 2.

Transmission electron microscopy. Duodenal biopsy samples were immediately fixed using 2.5% glutaraldehyde in 0.1 mol/L sodium cacodylate (pH 7.4) and stored at 4°C until processed. The tissues then were fixed with a secondary fixative, 1% osmium tetroxide in 0.1 mol/L sodium cacodylate (pH 7.4) for 1 hour at room temperature, washed repeatedly in distilled deionized water, dehydrated with a graded series of ethanol, and embedded in Embed 812 resin (Electron Microscopy Sciences, Hatfield, PA). Thick sections (0.5 μm) were stained with 1% toluidine blue and examined by light microscopy to confirm tissue orientation. Thin sections (80 nm) were cut on a Leica (Leica Microsystems Inc, Buffalo Grove, IL) UC6 ultramicrotome and stained with 2% uranyl acetate and lead citrate. Images were either acquired on a Tecnai T20 transmission electron microscope (FEI, Hillsboro, OR) equipped with an LaB6 source and operating at 100 kV, or a CM-100 transmission electron microscope (FEI/Philips, Hillsboro, OR) operating at 80 kV. Intact enterocytes were examined for the presence of CLDs (40–63 enterocytes/sample, 5 or 12 samples/group). Quantitative analyses were performed on enterocytes containing CLDs. The number of CLDs per enterocyte was counted and the diameters of individual CLDs were measured using ImageJ software (NIH, Bethesda, MD). Measured diameters were used to estimate the area of individual CLDs (area = π (diameter/2)^2), and the total CLD area per enterocyte was estimated by multiplying the average CLD area by the average CLD number. Qualitative assessments of lipids within the secretory pathway (ER, Golgi, and secretory vesicles) were made with a ranking system. Because it was too difficult to determine quantitatively the area of lipids within the secretory pathway, an in-house ranking system was used to arbitrarily classify each enterocyte as containing high, moderate, or low lipid content. Individual enterocytes were classified as containing low, moderate, or high amounts of secretory lipid, and then this information was used to assign each biopsy sample an overall ranking of low, moderate, or high. Previous electron microscopic analyses of intestinal lipid stores were used as a reference for the identification of intestinal lipid storage pools in the current study.[41–45]

Sample preparation for liquid chromatography–mass spectrometry/mass spectrometry analysis. Biopsy samples were washed once with 100 μL purified water followed by 100 μL washes using 100 mmol/L ammonium bicarbonate until the supernatant was clear, to remove the presence of blood in some samples. Tissue samples then were placed into 2-mL reinforced tubes containing 2.8-mm ceramic (zirconium oxide) beads (Cayman Chemical, Ann Arbor, MI). A total of 200 μL of 100 mmol/L ammonium bicarbonate was added to each sample, and the tubes were loaded into a Precellys 24 homogenizer (Berlin Instruments, Rockville, MD). The tissue was homogenized at 6500 rpm using 3 cycles of 20 seconds each. Protein concentrations were determined for each of the tissue solutions using a Pierce BCA assay kit (Thermo Scientific, Waltham, MA). An aliquot containing 100 μg protein was taken for processing. Before the digestion, the protein was precipitated and concentrated from solution using acetone. After drying the precipitated pellets, the protein samples were reduced using 10 mmol/L 1,4-dithiothreitol followed by alkylation using iodoethanol. Sequence grade Lys-C/Trypsin (Promega, Madison, WI) was used to enzymatically digest the protein samples in the Barocycler NEP2320 (Pressure Biosciences, Inc, Easton, MA) at 50°C under 20,000 psi for 1 hour. Digested samples were cleaned using C18 spin columns (Nest Group, Southborough, MA) and dried. Resulting pellets were resuspended in 97% purified water/3% acetonitrile/0.1% formic acid before liquid chromatography/mass spectrometry analysis.

Liquid chromatography–mass spectrometry/mass spectrometry. Digested samples were analyzed using the Dionex UltiMate 3000 RSLC Nano System coupled to a Q Exactive HF Hybrid Quadrupole-Orbitrap Mass Spectrometer (Thermo Fisher Scientific). Peptides generated during the digestion were loaded onto a 300 μm inner diameter $\times$ 5 mm C18 PepMap 100 (Thermo Fisher Scientific) trap column and washed with 98% purified water/2% acetonitrile/0.01% formic acid using a flow rate of 5 μL/min. The trap column was switched in-line with the analytical column after 5 minutes, and peptides were separated over a 75 μm $\times$ 150 mm reverse-phase Acclaim PepMap RSLC C18 analytical column using a 120-minute method at a flow rate of 300 nL/min. Mobile phase A contained 0.01% formic acid in water and mobile phase B consisted of 0.01% formic acid in 80% acetonitrile. The linear gradient began at 5% B and reached 30% B in 80 minutes, 45% B in 91 minutes, and 100% B in 93 minutes. The column was held at 100% B for the next 5 minutes before returning to 5% B, where it was equilibrated for 20 minutes. Samples were injected into the QE HF through the Nanospray Flex Ion Source fitted with a stainless-steel emission tip (Thermo Scientific). Data acquisition was performed by monitoring the top 20 precursors at 120,000 resolution with an injection time of 100 ms.

Proteomic data analysis. The results from the mass spectrometer were processed using the MaxQuant (Max-Planck Institute for Biochemistry, Martinsried, Germany) computational proteomics platform.[46] The peak list generated was searched against the Homo sapiens sequences from UniProt and a common contaminants database. The following settings were used for the MaxQuant run: trypsin and Lys-C digestion enzymes with 2 missed cleavages allowed, ethanolyl addition to cysteine as a fixed modification, N-terminal acetylation and oxidation of methionine as variable modifications, with 3 modifications allowed for each peptide, default Orbitrap parameters, minimum peptide length of 7 amino acids, label-free quantification was selected, match between runs was selected and the interval was set to 1 minute, and the protein false-discovery rate was set to 1%. An in-house script was used to perform the following on the MaxQuant results: remove all of the contaminant proteins, log transform ($\log_2$[x]) the label-free quantification intensity values, and input missing values using half of the highest intensity when all the values for a given protein were missing in 1 group and present in at least 3 samples of the other group. Only proteins that were identified in at least 3 samples in 1 treatment group were considered present in the duodenal biopsy samples. Only the relative label-free quantification values of proteins that were identified in at least 3 samples in both treatment groups, or identified in at least 3 samples in 1 treatment group and 0 samples in the other treatment group (imputed values used) were compared statistically. The statistical analyses were performed in the R environment (www.cran.r-project.org). A t test was performed on the label-free quantification intensities, with a P value $< .05$ considered a statistically significant difference between the groups. The differentially present proteins were classified into broad groups based on GO terms for biological process or molecular function using the Database for Annotation, Visualization, and Integrated Discovery version 6.7 and the UniProt database. Proteins with GO terms related to lipid (TG, phospholipid, cholesterol, and fatty acid) metabolism, lipoprotein metabolism and transport, and CLD storage and metabolism were identified and classified using the Database for Annotation, Visualization, and Integrated Discovery functional annotation clustering and functional annotation tables as well as the UniProt database. Protein–protein interactions were visualized with Search Tool for the Retrieval of Interacting Genes/Proteins version 10.5 using the confidence view (high confidence, score 0.700).

Statistical analysis. Data are presented as means $\pm$ SE. Plasma glucose concentrations, plasma TG concentration vs time curves, and lipoprotein fractions (TRL, CM, and VLDL) were compared using repeated-measures analysis of variance with post hoc analysis using a paired t test. Mean CLD numbers, diameters, and areas were compared using a t test. CLD diameter distribution was compared with the Kolmogorov–Smirnov test. Secretory lipids were assessed using a Fisher exact test.

References

1. Lewis GF, Xiao C, Hegele RA. Hypertriglyceridemia in the genomic era: a new paradigm. Endocr Rev 2015; 36:131147.
2. Mansbach CM, Siddiqi SA. The biogenesis of chylomicrons. Annu Rev Physiol 2010;72:315–333.

3. Dash S, Xiao C, Morgantini C, Lewis GF. New insights into the regulation of chylomicron production. Annu Rev Nutr 2015;35:265–294.
4. Xiao C, Stahel P, Carreiro AL, Buhman KK, Lewis GF. Recent advances in triacylglycerol mobilization by the gut. Trends Endocrinol Metab 2018;29:151–163.
5. Cohn JS, McNamara JR, Krasinski SD, Russell RM, Schaefer EJ. Role of triglyceride-rich lipoproteins from the liver and intestine in the etiology of postprandial peaks in plasma triglyceride concentration. Metabolism 1989;38:484–490.
6. Fielding BA, Callow J, Owen RM, Samra JS, Matthews DR, Frayn KN. Postprandial lipemia: the origin of an early peak studied by specific dietary fatty acid intake during sequential meals. Am J Clin Nutr 1996; 63:36–41.
7. Mattes RD. Brief oral stimulation, but especially oral fat exposure, elevates serum triglycerides in humans. Am J Physiol Gastrointest Liver Physiol 2009;296:G365–G371.
8. Chavez-Jauregui RN, Mattes RD, Parks EJ. Dynamics of fat absorption and effect of sham feeding on postprandial lipema. Gastroenterology 2010;139:1538–1548.
9. Robertson MD, Parkes M, Warren BF, Ferguson DJP, Jackson KG, Jewell DP, Frayn KN. Mobilisation of enterocyte fat stores by oral glucose in humans. Gut 2003;52:834–839.
10. Zhu J, Lee B, Buhman KK, Cheng J-X. A dynamic, cytoplasmic triacylglycerol pool in enterocytes revealed by ex vivo and in vivo coherent anti-Stokes Raman scattering imaging. J Lipid Res 2009;50:1080–1089.
11. Takahara E-I, Mantani Y, Udayanga KGS, Qi W-M, Tanida T, Takeuchi T, Yokoyama T, Hoshi N, Kitagawa H. Ultrastructural demonstration of the absorption and transportation of minute chylomicrons by subepithelial blood capillaries in rat jejunal villi. J Vet Med Sci 2013; 75:1563–1569.
12. Hung Y-H, Carreiro AL, Buhman KK. Dgat1 and Dgat2 regulate enterocyte triacylglycerol distribution and alter proteins associated with cytoplasmic lipid droplets in response to dietary fat. Biochim Biophys Acta 2017; 1862:600–614.
13. Beilstein F, Bouchoux J, Rousset M, Demignot S. Proteomic analysis of lipid droplets from Caco-2/TC7 enterocytes identifies novel modulators of lipid secretion. PLoS One 2013;8:e53017.
14. D'Aquila T, Sirohi D, Grabowski JM, Hedrick VE, Paul LN, Greenberg AS, Kuhn RJ, Buhman KK. Characterization of the proteome of cytoplasmic lipid droplets in mouse enterocytes after a dietary fat challenge. PLoS One 2015; 10:e0126823.
15. Uchida A, Whitsitt MC, Eustaquio T, Slipchenko MN, Leary JF, Cheng J-X, Buhman KK. Reduced triglyceride secretion in response to an acute dietary fat challenge in obese compared to lean mice. Front Physiol 2012;3:26.
16. Beilstein F, Carriere V, Leturque A, Demignot S. Characteristics and functions of lipid droplets and associated proteins in enterocytes. Exp Cell Res 2015;340:172–179.
17. D'Aquila T, Hung Y-H, Carreiro A, Buhman KK. Recent discoveries on absorption of dietary fat: presence, synthesis, and metabolism of cytoplasmic lipid droplets within enterocytes. Biochim Biophys Acta 2016; 1861:730–747.
18. Fielding BA, Reid G, Grady M, Humphreys SM, Evans K, Frayn KN. Ethanol with a mixed meal increases postprandial triacylglycerol but decreases postprandial nonesterified fatty acid concentrations. Br J Nutr 2000; 83:597–604.
19. Dash S, Xiao C, Morgantini C, Connelly PW, Patterson BW, Lewis GF. Glucagon-like peptide-2 regulates release of chylomicrons from the intestine. Gastroenterology 2014;147:1275–1284.
20. Evans K, Kuusela PJ, Cruz ML, Wilhelmova I, Fielding BA, Frayn KN. Rapid chylomicron appearance following sequential meals: effects of second meal composition. Br J Nutr 1998;79:425–429.
21. Lewis GF, Carpentier A, Adeli K, Giacca A. Disordered fat storage and mobilization in the pathogenesis of insulin resistance and type 2 diabetes. Endocr Rev 2002; 23:201–229.
22. Westberg-Rasmussen S, Starup-Linde J, Hermansen K, Holst JJ, Hartmann B, Vestergaard P, Gregersen S. Differential impact of glucose administered intravenously or orally on bone turnover markers in healthy male subjects. Bone 2017;97:261–266.
23. Hartmann B, Harr MB, Jeppesen PB, Wojdemann M, Deacon CF, Mortensen PB, Holst JJ. In vivo and in vitro degradation of glucagon-like peptide-2 in humans. J Clin Endocrinol Metab 2000;85:2884–2888.
24. Xiao C, Bandsma RH, Dash S, Szeto L, Lewis GF. Exenatide, a glucagon-like peptide-1 receptor agonist, acutely inhibits intestinal lipoprotein production in healthy humans. Arterioscler Thromb Vasc Biol 2012; 32:1513–1519.
25. Couture P, Tremblay AJ, Kelly I, Lemelin V, Droit A, Lamarche B. Key intestinal genes involved in lipoprotein metabolism are downregulated in dyslipidemic men with insulin resistance. J Lipid Res 2014; 55:128–137.
26. Bourassa S, Fournier F, Nehmé B, Kelly I, Tremblay A, Lemelin V, Lamarche B, Couture P, Droit A. Evaluation of iTRAQ and SWATH-MS for the quantification of proteins associated with insulin resistance in human duodenal biopsy samples. PLoS One 2015;10:e0125934.
27. Yanase H, Shimizu H, Kanda T, Fujii H, Iwanaga T. Cellular localization of the diazepam binding inhibitor (DBI) in the gastrointestinal tract of mice and its coexistence with the fatty acid binding protein (FABP). Arch Histol Cytol 2001;64:449–460.
28. Ahmed MY, Al-Khayat A, Al-Murshedi F, Al-Futaisi A, Chioza BA, Pedro Fernandez-Murray J, Self JE, Salter CG, Harlalka GV, Rawlins LE, Al-Zuhaibi S, Al-Azri F, Al-Rashdi F, Cazenave-Gassiot A, Wenk MR, Al-Salmi F, Patton MA, Silver DL, Baple EL, McMaster CR, Crosby AH. A mutation of EPT1 (SELENOI) underlies a new disorder of Kennedy pathway phospholipid biosynthesis. Brain J Neurol 2017;140:547–554.
29. Payne F, Lim K, Girousse A, Brown RJ, Kory N, Robbins A, Xue Y, Sleigh A, Cochran E, Adams C, Dev Borman A, Russel-Jones D, Gorden P, Semple RK, Saudek V, O'Rahilly S, Walther TC, Barroso I,

Savage DB. Mutations disrupting the Kennedy phosphatidylcholine pathway in humans with congenital lipodystrophy and fatty liver disease. Proc Natl Acad Sci U S A 2014;111:8901–8906.
30. van der Veen JN, Kennelly JP, Wan S, Vance JE, Vance DE, Jacobs RL. The critical role of phosphatidylcholine and phosphatidylethanolamine metabolism in health and disease. Biochim Biophys Acta 2017;1859:1558–1572.
31. Itabe H, Yamaguchi T, Nimura S, Sasabe N. Perilipins: a diversity of intracellular lipid droplet proteins. Lipids Health Dis 2017;16:83.
32. Jaishy B, Abel ED. Lipids, lysosomes, and autophagy. J Lipid Res 2016;57:1619–1635.
33. Zhang W, Lilja L, Mandic SA, Gromada J, Smidt K, Janson J, Takai Y, Bark C, Berggren P-O, Meister B. Tomosyn is expressed in beta-cells and negatively regulates insulin exocytosis. Diabetes 2006;55:574–581.
34. Zhu Q, Yamakuchi M, Ture S, de la Luz Garcia-Hernandez M, Ko KA, Modjeski KL, LoMonaco MB, Johnson AD, O'Donnell CJ, Takai Y, Morrell CN, Lowenstein CJ. Syntaxin-binding protein STXBP5 inhibits endothelial exocytosis and promotes platelet secretion. J Clin Invest 2014;124:4503–4516.
35. Mansbach CM, Siddiqi S. Control of chylomicron export from the intestine. Am J Physiol Gastrointest Liver Physiol 2016;310:G659–G668.
36. Fagerberg L, Hallström BM, Oksvold P, Kampf C, Djureinovic D, Odeberg J, Habuka M, Tahmasebpoor S, Danielsson A, Edlund K, Asplund A, Sjöstedt E, Lundberg E, Szigyarto CA-K, Skogs M, Takanen JO, Berling H, Tegel H, Mulder J, Nilsson P, Schwenk JM, Lindskog C, Danielsson F, Mardinoglu A, Sivertsson A, von Feilitzen K, Forsberg M, Zwahlen M, Olsson I, Navani S, Huss M, Nielsen J, Ponten F, Uhlén M. Analysis of the human tissue-specific expression by genome-wide integration of transcriptomics and antibody-based proteomics. Mol Cell Proteomics 2014;13:397–406.
37. Persson B, Kallberg Y, Bray JE, Bruford E, Dellaporta SL, Favia AD, Duarte RG, Jörnvall H, Kavanagh KL, Kedishvili N, Kisiela M, Maser E, Mindnich R, Orchard S, Penning TM, Thornton JM, Adamski J, Oppermann U. The SDR (short-chain dehydrogenase/reductase and related enzymes) nomenclature initiative. Chem Biol Interact 2009;178:94–98.
38. Oppermann UC, Filling C, Jörnvall H. Forms and functions of human SDR enzymes. Chem Biol Interact 2001;130–132:699–705.
39. Lemieux S, Fontani R, Uffelman KD, Lewis GF, Steiner G. Apolipoprotein B-48 and retinyl palmitate are not equivalent markers of postprandial intestinal lipoproteins. J Lipid Res 1998;39:1964–1971.
40. Booth CC, Read AE, Jones E. Studies on the site of fat absorption: 1. The sites of absorption of increasing doses of I-labelled triolein in the rat. Gut 1961;2:23–31.
41. Cardell RR, Badenhausen S, Porter KR. Intestinal triglyceride absorption in the rat. An electron microscopical study. J Cell Biol 1967;34:123–155.
42. Friedman HI, Cardell RR. Effects of puromycin on the structure of rat intestinal epithelial cells during fat absorption. J Cell Biol 1972;52:15–40.
43. Sabesin SM, Frase S. Electron microscopic studies of the assembly, intracellular transport, and secretion of chylomicrons by rat intestine. J Lipid Res 1977;18:496–511.
44. Young SG, Cham CM, Pitas RE, Burri BJ, Connolly A, Flynn L, Pappu AS, Wong JS, Hamilton RL, Farese RV. A genetic model for absent chylomicron formation: mice producing apolipoprotein B in the liver, but not in the intestine. J Clin Invest 1995;96:2932–2946.
45. Jersild RA. A time sequence study of fat absorption in the rat jejunum. Am J Anat 1966;118:135–162.
46. Cox J, Mann M. MaxQuant enables high peptide identification rates, individualized p.p.b.-range mass accuracies and proteome-wide protein quantification. Nat Biotechnol 2008;26:1367–1372.

Received May 18, 2018. Accepted October 5, 2018.

Correspondence
Address correspondence to: Gary F. Lewis, MD, FRCPC, Toronto General Hospital, 200 Elizabeth Street, EN12-218, Toronto, Ontario, M5G 2C4 Canada. e-mail: gary.lewis@uhn.ca; fax: (416) 340-3314.

Author contributions
Changting Xiao, Satya Dash, and Gary F. Lewis were responsible for the study concept and design; Changting Xiao, Priska Stahel, Alicia L. Carreiro, Yu-Han Hung, and Ian Bookman performed data acquisition; Changting Xiao, Priska Stahel, Alicia L. Carreiro, Satya Dash, Kimberly K. Buhman, and Gary F. Lewis analyzed and interpreted data; Changting Xiao and Gary F. Lewis wrote the manuscript; Changting Xiao, Priska Stahel, Alicia L. Carreiro, Satya Dash, Kimberly K. Buhman, and Gary F. Lewis revised the manuscript and were responsible for important intellectual content; and Gary F. Lewis obtained funding and performed study supervision.

Conflicts of interest
The authors disclose no conflicts.

Funding
This work was supported by an operating grant from the Canadian Institutes of Health Research; the Drucker Family Chair in Diabetes Research and the Sun Life Financial Chair in Diabetes (G.F.L.); a Banting and Best Diabetes Centre Hugh Sellers Postdoctoral Fellowship and a Diabetes Action Canada Postdoctoral Fellowship (P.S.); a Purdue Research Foundation Fellowship and a Purdue Bilsland Dissertation Fellowship (A.L.C.); and a Diabetes Canada New Investigator grant and the Reuben and Helene Dennis Scholarship from the Banting and Best Diabetes Centre (S.D.).